N72-28896

BOEING DOCUMENT
D180-15006-1

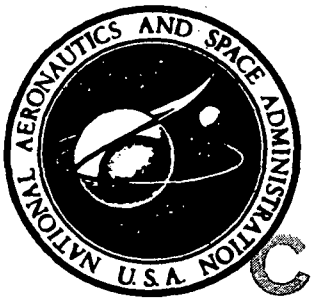

Final Report

FUNDAMENTAL INVESTIGATION OF STRESS CORROSION CRACKING

By

T. R. Beck, M. J. Blackburn & W. H. Smyrl

Prepared for

NATIONAL AERONATUCS AND SPACE ADMINISTRATION
HEADQUARTERS
Contract NASW-2245

THE BOEING COMPANY

CONTRACT NASW-2245

FUNDAMENTAL INVESTIGATION OF STRESS CORROSION CRACKING

Final Report
Covering work done in the
Period of

July 1, 1971 through April 30, 1972

Prepared by

T. R. Beck, M. J. Blackburn and W. H. Smyrl

Structures and Materials Research
Aerospace Group

THE BOEING COMPANY
Seattle, Washington 98124

TABLE OF CONTENTS

1.0 SUMMARY

Two principle areas studied on this contract were stress corrosion crack growth rates of a titanium alloy in liquid environments containing halide ions and pitting corrosion of titanium in bromide solutions. Examination of the simpler pitting process gives some new insights into the electrochemistry of stress corrosion cracking.

Crack Growth in Liquid Environments Containing Halide Ions

The question that this work attempted to answer was "what is the rate limiting process that controls the rate of region II (plateau) velocites observed in many titanium:environment couples during SCC?" Two initial assumptions were made, that the rate of propagation was controlled by a macroscopic solution parameter and that this parameter was viscosity. A series of solutions were prepared using lithium chloride as the solute and water, methanol, glycerin, formic acid, acetone, dimethyl sulphoxide, etc. as solvents, these solutions were prepared with a 5:1 solvent-solute ratio. Viscosity was varied by changing the temperature and it was found that:

- in all solvents the velocity of cracking was proportional to the reciprocal of the viscosity;
- each solvent gave a separate relationship;
- the temperature dependence and numerical values for the apparent activation energy of cracking and viscosity were the same.

Various other parameters were studied in an attempt to obtain a single relationship for all solvents or to account for the differences between solvents. It was found that a conductivity;crack-velocity correlation existed for all solutions over a wide range of values. However, differences could also be attributed to potential and chemical effects. Detailed evaluation of the results lead to the conclusion that although some surprising good relationships were established no simple explanation based on fluid flow or various types of chemical reactions could account for all the results. Several other

experiments grew from the main program which resulted in a much improved knowledge of the influence of potential, pH and temperature on crack velocity in aqueous halide solutions.

Pitting of Titanium

Small diameter titanium rods were cast in epoxy resin rods like a pencil . Pitting corrosion on one end with anode facing up gives uniform current distribution and conditions in the electrolyte applicable to one-dimensional analysis of mass transport. Current-potential curves, morphology of the corroding surface, gas analysis, valence of titanium, potential gradients in the pit electrolyte, and open-circuit potential transients were studied in bromide solutions. The evidence indicates that titanium dissolves at close to the reversible potential for Ti(IV) and that a salt film covers the metal surface.

2.0 INTRODUCTION

This is the final report on the fundamental investigation of stress corrosion cracking of titanium in this series of NASA/Headquarters contracts at The Boeing Company. Studies of stress corrosion cracking were initiated at the Boeing Scientific Research Laboratories in 1965 (1) and continued under NASA sponsorship beginning July 1966 (2). Work from July 1966 through June 1971 was contract NAS7-489 (3). The present report summarizes work completed in the period of July 1, 1971 through April 1972 on contract NASW-2244. Brief letter reports were submitted on a quarterly bases.

3.0 REFERENCES

1. Beck, T. R., Boeing Document D1-82-0554, July 1966.
2. Beck, T. R., and Blackburn, M. J., Research Proposal D1-82-0467, August 1965.
3. Beck, T. R., Contract NAS7-489, Quarterly Progress Reports No. 1, September 1966 through No. 20, July 1971.

4.0 TECHNICAL DISCUSSION

4.1 STRESS CORROSION CRACKING OF A TITANIUM ALLOY IN CHLORIDE CONTAINING LIQUID ENVIRONMENTS

INTRODUCTION

Stress corrosion cracking (SCC) of titanium alloys, or any material, is a complex subject-- for example, the scale (size) that one may examine the problem ranges from the failure of large structures to atomistic descriptions of events at a propagating crack tip. In recent comprehensive reviews (1,2) the range of the subject was demonstrated and it was shown that the myriad variables render any really complete and quantitative description of SCC unlikely at least in the near future. Thus, in selecting any aspect of the problem the contraints on experimental and theoretical analyses emerging from the investigation must be realized. The work which is described in this paper is an attempt to explain the controlling factors that determine the plateau velocity of a stress corrosion crack in some systems. The origin of this problem can be understood by examination of Figure 1 which illustrates the extensive range of plateau velocities which may be observed in one heat treatment condition of one alloy. It is noted that the environments contain liquids and gases, and in fact, if results for cadmium embrittlement (3) were present could also include solid environments. Contemplation of Figure 1 raised the obvious question of the factor(s) that controlled the plateau velocity and the point was selected as being worthy of further study. It was clear that one single physical property could not form the basis of an explanation of growth velocity-- for example, it is difficult to see the connection (if any) between liquid mercury, molten halide salts and hydrogen gas. Thus, an initial restriction was placed on the range of these experiments and this paper only considers cracking in fluid environments.

It was considered that viscosity could at least provide a partial correlation in liquid environments although there was little evidence in the literature to support this guess. Sedriks (4) had shown that the time to failure of smooth specimens of titanium tested in a series of alcohols containing iodine could be correlated with the viscosity of the solution. Beck, et al., (5) had also shown that the velocity of cracking in water-glycerol-HCl mixtures

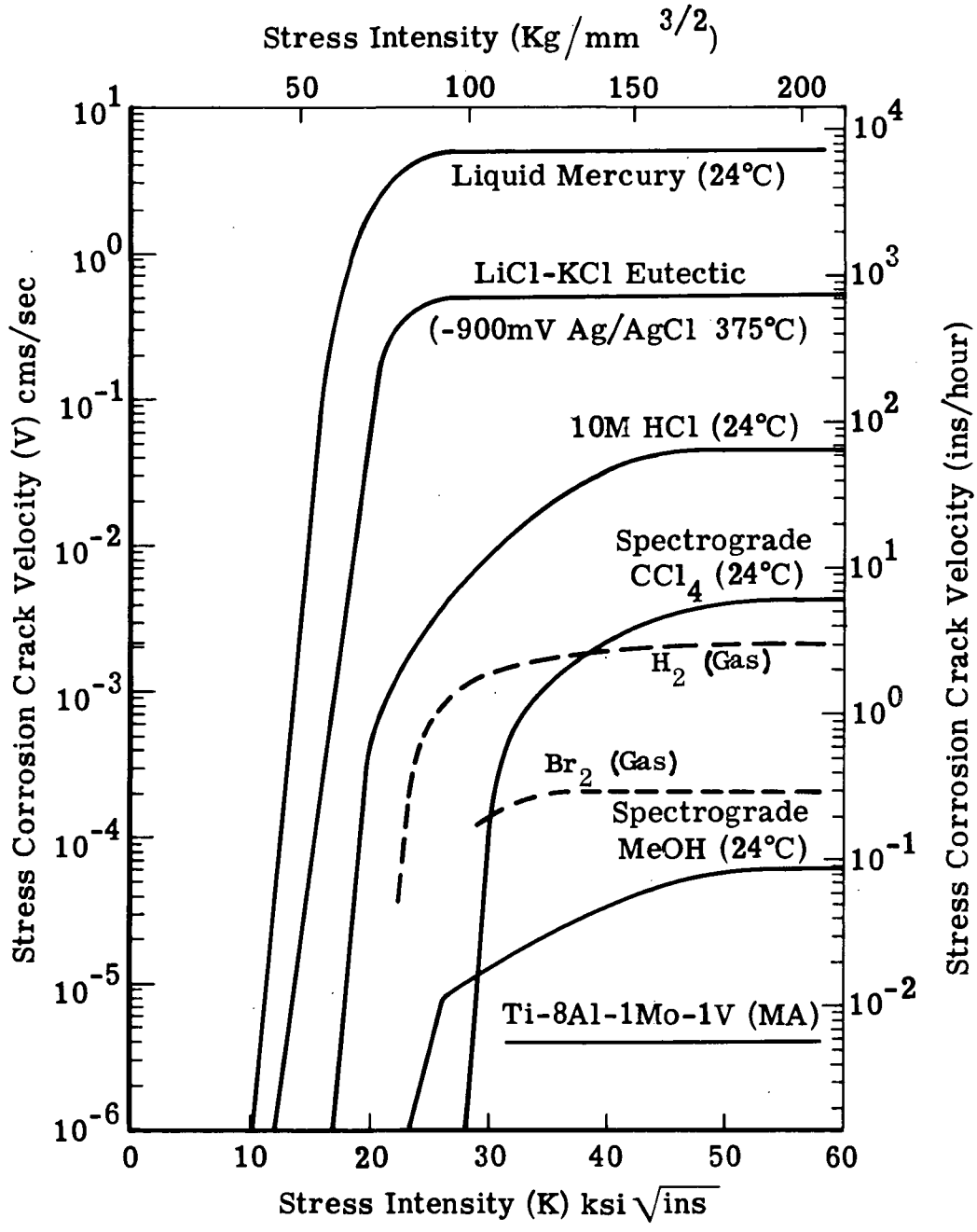

Fig. 1 - Crack velocity (V) vs. stress intensity (K) for Ti-8Al-1Mo-1V (Mill Annealed) tested in a variety of environments and illustrating the wide range of plateau (Region II) velocities observed. Note that by using a different heat treatment the velocity range could be extended to cover about eight orders of magnitude [Ref. 1].

varied as the viscosity to the half power. These results showed if nothing else that viscosity was indeed a variable. It was considered at the inception of this program that viscosity could control velocity in several ways of which the most probable were:

- fluid flow within the crack cavity;
- through its influence on mass transport processes by affecting values of the diffusion coefficient ($\mathcal{D}$) or conductivity (κ).

During the course of this study several other points such as the influence of concentration of halide ions and potential effects were investigated. A brief description of these results are included to elaborate on some of the statements made in Refs. 1 and 2. It should be noted that in any investigation that purports to study the influence of a variable such as concentration, temperature, etc., one should consider the viscosity changes produced by varying the test conditions.

An additional complication in alloy selection became clear during the course of this study. The alloy selected was Ti-8Al-1Mo-1V which is renowned throughout the stress corrosion world for its splendid susceptibility to SCC. The degree of susceptibility for any alloy is best demonstrated in practice by the position of a velocity (V) versus applied stress intensity (K) in the V:K plane, which defines both the plateau velocity and the stress intensity value below which cracking will not occur, K_{1SCC}. It is well established that the presence of Cl^-, Br^- and I^- ions in aqueous solutions either induce cracking or accelerate cracking with respect to any crack growth that occurs in an inert environment.* The latter form of crack growth, first reported by Sandoz (6), may be due to residual hydrogen in the metal or a creep type failure. In the alloy Ti-8Al-1Mo-1V this (inert environment) form of crack growth is strongly dependent upon heat treatment and the variation is

---

* Such crack growth in inert environments does not occur in all alloys. For example, it is prevalent in the alloy Ti-8Al-1Mo-1V but is rare in Ti-4Al-3Mo-1V. The extent appears to be related to the hydrogen content of the alloy (6,7).

represented semischematically in Figure 2. It can be seen that in the lowest toughness condition the difference between the salt solution and an inert environment is at a minimum but the difference increases as the rate of cooling from the solution treatment temperature in the $\alpha+\beta$ region increases. The behavior of the sheet of Ti-8Al-1Mo-1V selected for this study was similar to that shown in Figure 2. Unfortunately, an earlier study (see Ref. 1) indicates that after the 820°C, water quench treatment of the plate of Ti-8Al-1Mo-1V used, crack growth in inert environments at room temperature was extremely slow $>10^{-7}$ cm/sec. and this result was prematurely extrapolated to the present study. Crack growth in Ti-8Al-1Mo-1V alloy used in this study after the same heat treatment occurred at $\sim 10^{-6}$ cm/sec. in inert conditions.

As in all SCC experiments the experimental variables must be recognized and controlled. Thus in these tests:

- the alloy and heat treatment, specimen orientation, loading rate, etc. were constant
- the test solutions in the first part of the work described herein contained chloride or bromide ions added in the form of the lithium salt, but other solutions were studied later in the program. These solutions were prepared with a constant mole ratio - 1 mole of salt being added to 5 moles of the solvent.

4.1.1 Experimental Techniques

The techniques used are summarized briefly in the following sections. More complete descriptions may be found in Refs. 5 and 8.

Alloy--The Titanium-8Aluminum-1Vanadium-1Molydendum (Ti-8-1-1) was selected for this study as it had been widely studied both in this laboratory and by other workers. A sheet 0.25 inches thick was selected which showed an extreme transverse (0002)α texture which results in preferential crack propagation in the longitudinal direction. The heat treatment selected was 820°C for one hour and water quenched as this resulted in the occurrence crack extension over a wide range of K levels.

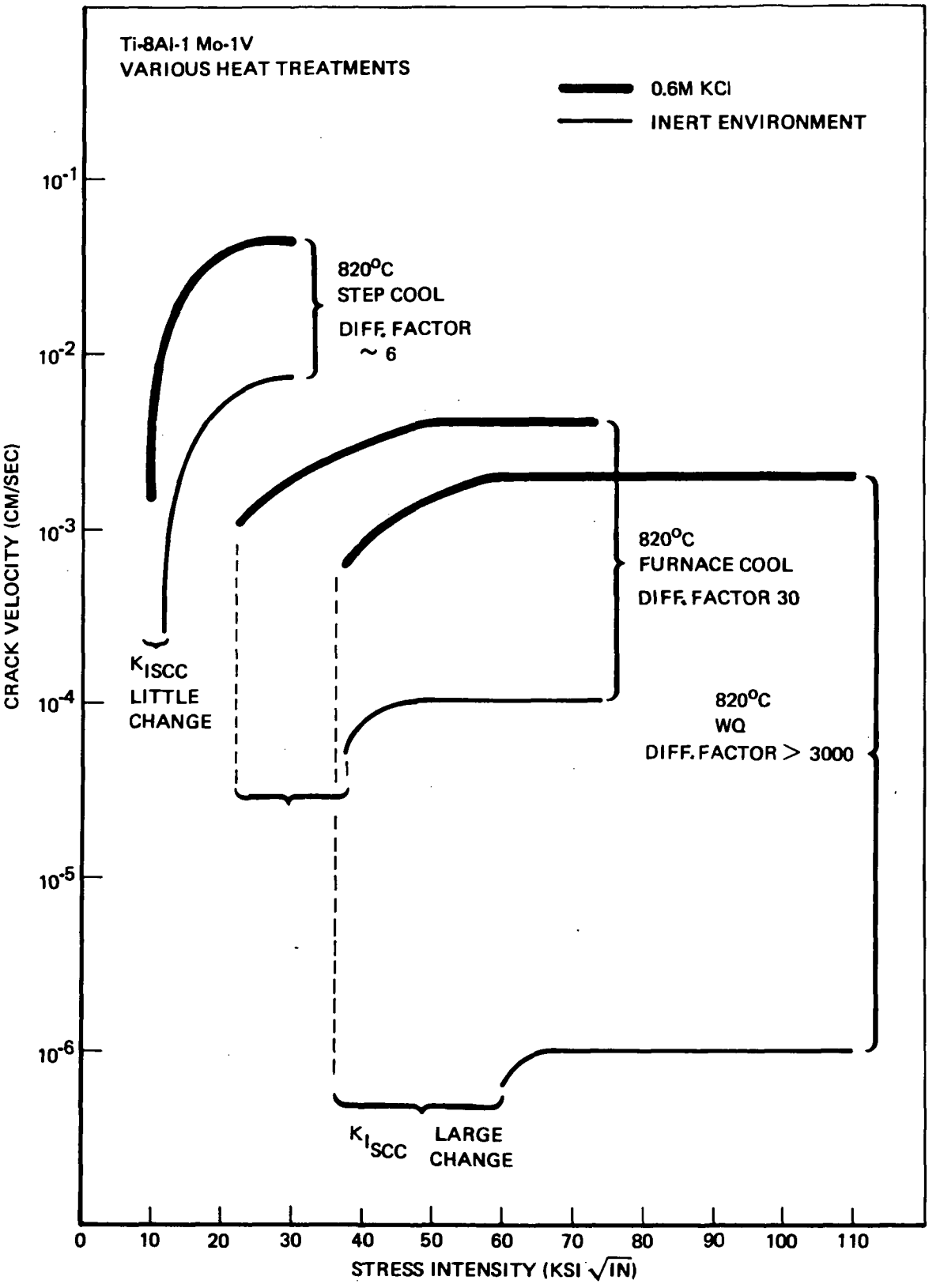

Fig. 2 - Crack velocity (V) vs. stress intensity (K) relationships for Ti-8Al-1Mo-1V tested in an aggressive (0.6 M KCl) and an inert (e.g., argon gas) environment. The relative displacements of the curve pairs is strongly dependent upon heat treatment. Note that the lower (inert atmosphere) curve places a limit on the range of crack velocities that can be obtained in any series of experiments (at the same test temperature).

Specimens--Double Cantilever Beam (DCB) specimens were cut from the sheet in the WR orientation. These were loaded to a constant deflection using wedges of a Ti-11% Mo alloy heat treated to a strength level of 180 ksi. The applied stress intensity levels were computed from the standard equation for this specimen (9). The specimen dimensions for these tests were one inch wide and five inches long, utilizing an initial crack length of 2.5 cm. Crack extension could be measured over a length of ∿5.0 centimeters.

Properties

Mechanical Properties--Yield strength 124 Ksi (87.2 Kg/mm^2), ultimate tensile strength 134 Ksi (94.2 Kg/mm^2), 15% elongation.

Fracture Toughness--90-100 $Ksi\sqrt{in}$, although this value is invalid as a plane strain fracture toughness value specimens did not comply with the thickness criteria of $t > 2.5(\frac{\sigma_Y}{K})^2$.

Microstructure--The heat treatment resulted in the conventional equiaxed $\alpha+\beta$ structure. There was no evidence of the α_2-phase within the α-phase.

Environments--A wide range of environments were studied in these experiments, these were prepared from analytical grade chemicals. The bulk of the experiments were conducted using solvent-halide mixtures usually in molar ratio of 5 solvent:1 solute (halide). The halide (chloride, bromide, iodine) was in the form of the acid or alkali metal salts.

Test Procedure--Tests were conducted at several temperatures between -70°C and 220°C, and the general technique was as follows. The solution in which the test was to be conducted was held at the required temperature ($\pm$4°C) in a constant temperature bath. Unloaded specimen were cooled or heated to approximately the same temperature, rapidly loaded and immersed in the solution. Crack extension was measured optically with reference to a grid scribed on the specimen surface. During the tests at open circuit the potential was monitored with reference to a room temperature saturated

calomel electrode (SCE). In tests performed under a controlled potential a Wenking potentiostat was used in conjunction with a platinum counter electrode and a room temperature SCE.

Physical Property Measurement--The viscosity of many of the solutions used in this program was measured using calibrated falling-ball or Ostwald viscometers. In some instances data from the literature was used. The conductivity of each solution was measured using an AC bridge with the normal capacitance compensation (10). The measurements were made at a fixed frequency of 1000 cycles/sec. The conductivity cell was calibrated with a 1.0 demal solution of KCl. The electrodes of the conductivity cell were bright platinum because it is known that some nonaqueous solvents (e.g., DMSO (11)) decompose at platinized-platinum electrodes.

4.1.2 Viscosity-Velocity Relationships

Lithium Chloride - Water

This environment was selected because of the wide range of temperatures (and viscosities) over which tests could be performed. Using the 1:5, $LiCl:H_2O$ mixture it was found that tests could not be performed below ∿-70°C due to precipitation of LiCl which occurred preferentially on the specimen. Tests were performed over the temperature range +112°C to -70°C in this solution. Some viscosity data for these solutions was obtained from Ref. (12) and some from Ref. (13) and the two were in excellent agreement where they overlapped. The variation of plateau velocity with temperature is shown in Figure 3, and shows a similar trend to the viscosity data. It is immediately apparent that the velocity does not show a linear relationship over this temperature range, and thus the apparent activation energy for the process is not constant-- in fact, the value varies from 4.4 Kcal/mole at the higher temperatures (∿80°C) to 8.4 at the lower temperatures (∿-50°C).
The apparent activation energy of the viscosity exhibits both a similar variation and approximately the same numerical values over this range (see (12)). Figure 4 shows the variation of the logarithm of the velocity of crack growth with the logarithm of the reciprocal of the viscosity which illustrates that

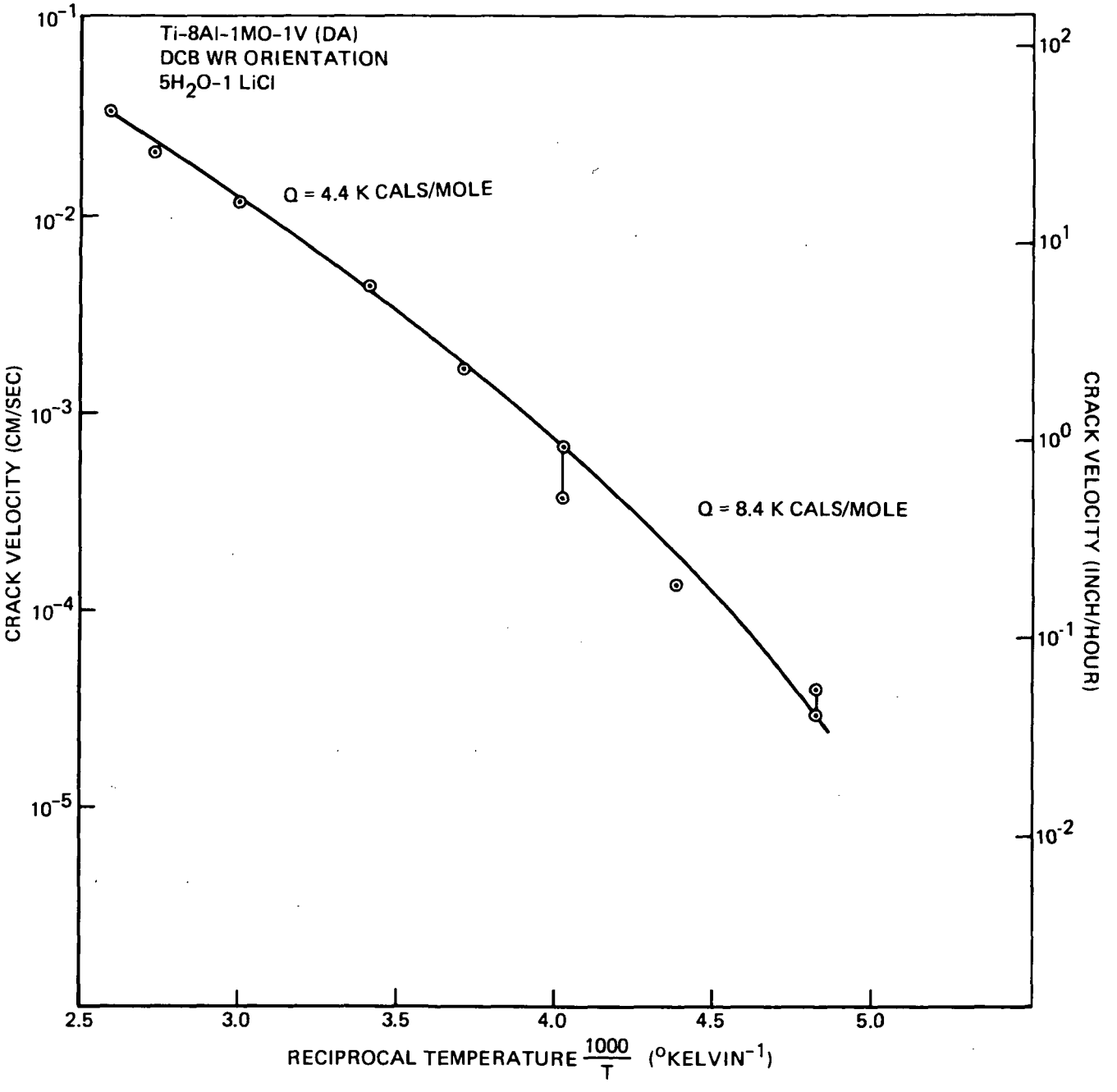

Fig. 3 - The variation of Region II (plateau) velocity with reciprocal temperature (°Kelvin) for Ti-8Al-1Mo-1V tested in 5:1 water: LiCl mole ratio mixtures.

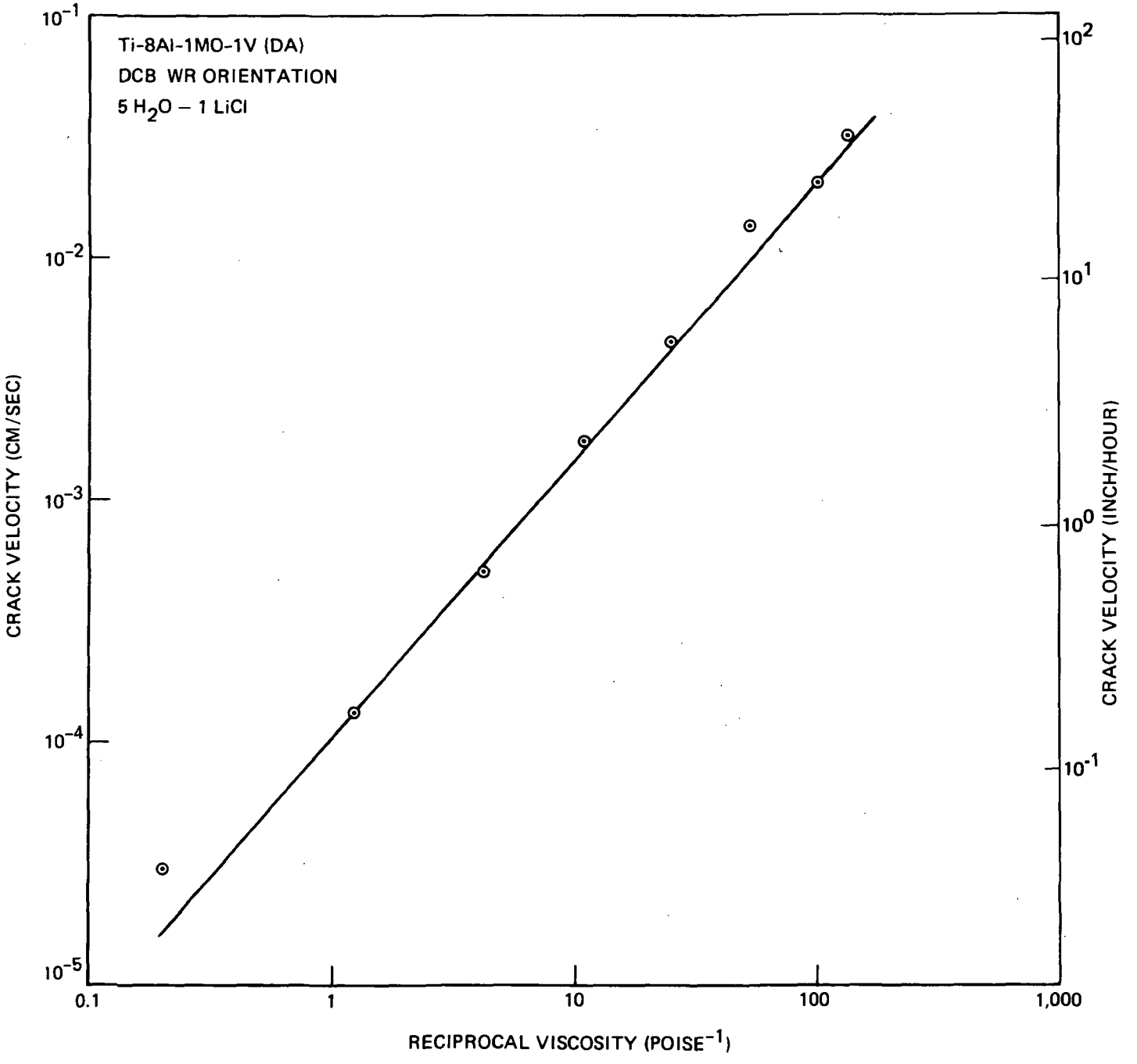

Fig. 4 - The variation of Region II (plateau) velocity with reciprocal viscosity ($1/\eta$) for Ti-8Al-1Mo-1V tested in 5:1, water: LiCl mole ratio mixtures.

a linear relationship is obtained with a slope of 1.14. A smaller number of tests was performed in which the halide ion or the action were different. Figure 4 includes data for LiBr-water and HCl-water solutions and it can be seen that these points are close to the LiCl-water results.

Other Solutions

Having obtained this relatively good correlation between velocity and viscosity the program was extended to include other solvents. The choice of such solvents was restricted by the requirement that the solubility of LiCl or LiBr had to be sufficiently high to produce a 5:1/solvent:solute solution. The following solvents were found to fulfill this requirement:

Methanol
Glycerine
Dimethyl Sulfoxide
HexamethylPhosphoric Triamide
N, N-DimethylAcetamide
Formic Acid (9% H_2O)
Acetone -Lithium Bromide ($t \geq 60°C$).

} Lithium Chloride

Before describing the results obtained in these solutions some of the experimentally imposed limitations should be noted. The methanol solutions could only be studied over a limited temperature range the upper limit ($\sim$60°C) being dictated by the evaporation rate of the methanol and the lower limit by the rapid fall in solubility of LiCl at temperatures below 20°C. Glycerine solutions could be utilized over a wider range of temperatures although some decomposition appeared to occur at temperatures >230°C. Some ambiguity was introduced using this solvent due to the absorption of water--this was minimized in these tests by using fresh glycerine (water content <0.1%) and by heating the solution to 210°C which appeared effective in removing water introduced with the LiCl. Dimethyl sulphoxide would not dissolve sufficient LiCl at room temperature to produce a 5:1 mole ratio and some tests were performed in 6:1 mole ratio solutions. However, at temperatures above $\sim$100°C 5:1 mole ratio solutions could be prepared and the supersaturated solution was stable on cooling to room temperature. The acetone solution also had a limited temperature range available for study

for the same reasons as the methanol: LiCl solutions. Tests in the other solutions were only performed at room temperature. Similar tests were performed in these solutions as those in the LiCl:water mixtures-- stress corrosion tests in which the plateau velocity was the parameter of interest coupled with viscosity (and conductivity) measurements on the solutions. The results of these tests are summarized in Figures 5 (a),(b) and (c), and the following points can be made although it should be recognized that the data are less numerous than those for LiCl-water mixtures.

- The apparent activation energies for the plateau velocity crack growth are ∿11 Kcals/mole for glycerine, ∿9 Kcals/mole for DMSO and ∿5 Kcals/mole for methanol;
- The apparent activation energies are similar to the activation energies of the viscosity in these temperature ranges (data not shown);
- The log viscosity-log reciprocal viscosity lie on two curves. Results in glycerine and methanol lie on the same curve which is parallel to but displaced downwards from the LiCl-water results. The results in acetone, DMSO, etc. lie on a line of similar slope displaced downward from the other curves.

LiCl:Water:Glycerine Solutions

In the above experiments the viscosity of the solutions was changed by varying the temperature. It was considered that an investigation of solutions in which the viscosity was varied at a constant temperature would provide useful confirmatory evidence for the data generated at this stage of the investigation. Thus, a series of tests were performed on LiCl-H_2O-glycerine mixtures-- these results are included in Figure 5(a) and it can be seen that these results do not conform with the results obtained in other solutions. In fact, over the viscosity range 0.1-1 poise the relationship between viscosity and velocity is very similar to that obtained in an earlier investigation in which a $\eta^{1/2}$ relationship was obtained (5). However, at very high viscosities the plateau velocity shows a much stronger viscosity dependence.

It is also of interest that the points lie above both the glycerine-LiCl and

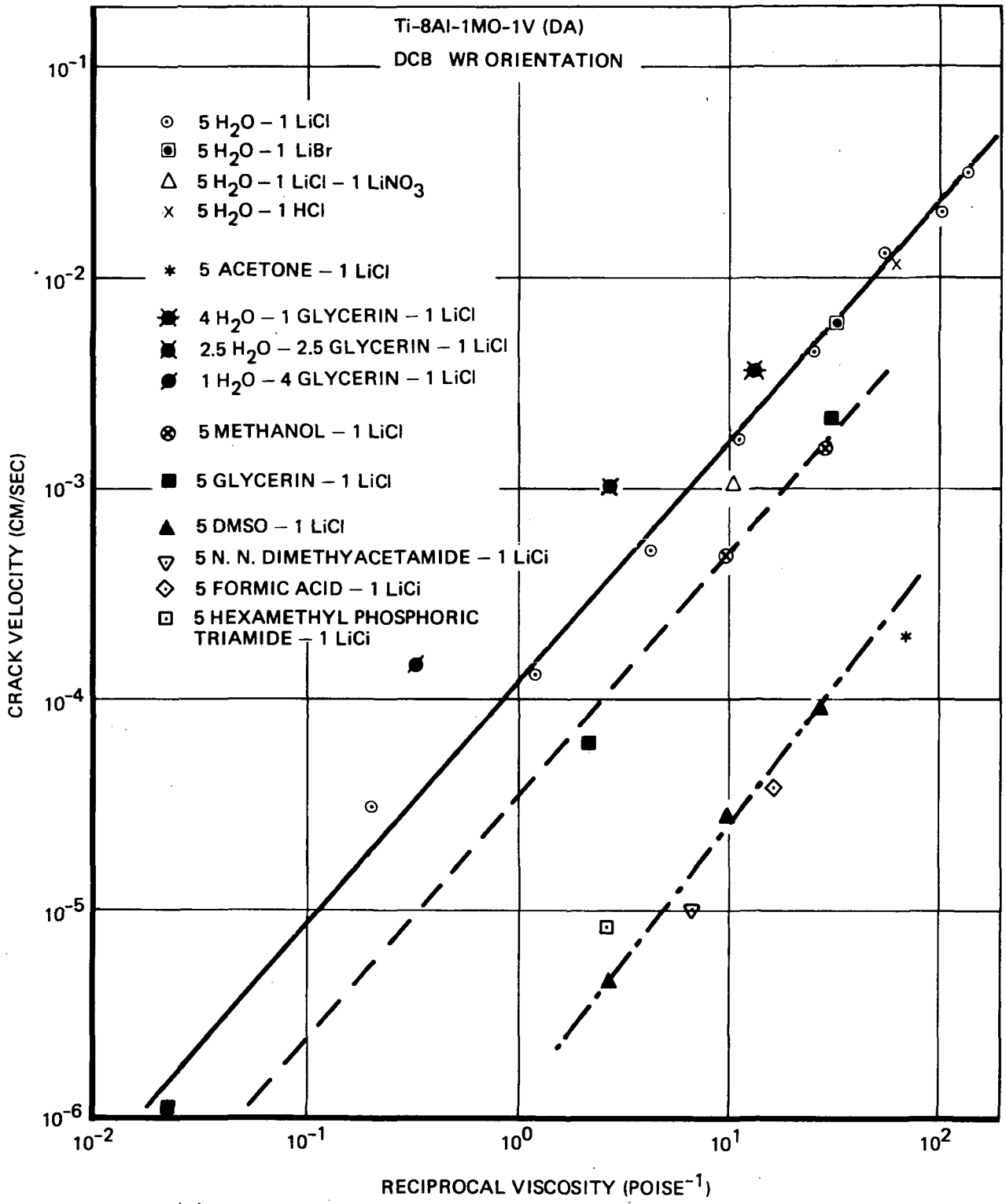

Fig. 5 - (a) Region II velocity variation with reciprocal viscosity (1/η) for Ti-8Al-1Mo-1V tested in a variety of solvent: halide mixtures. Note that three approximate straight line relationships are obtained and that the water-glycerine - LiCl results lie above the water and glycerine lines.

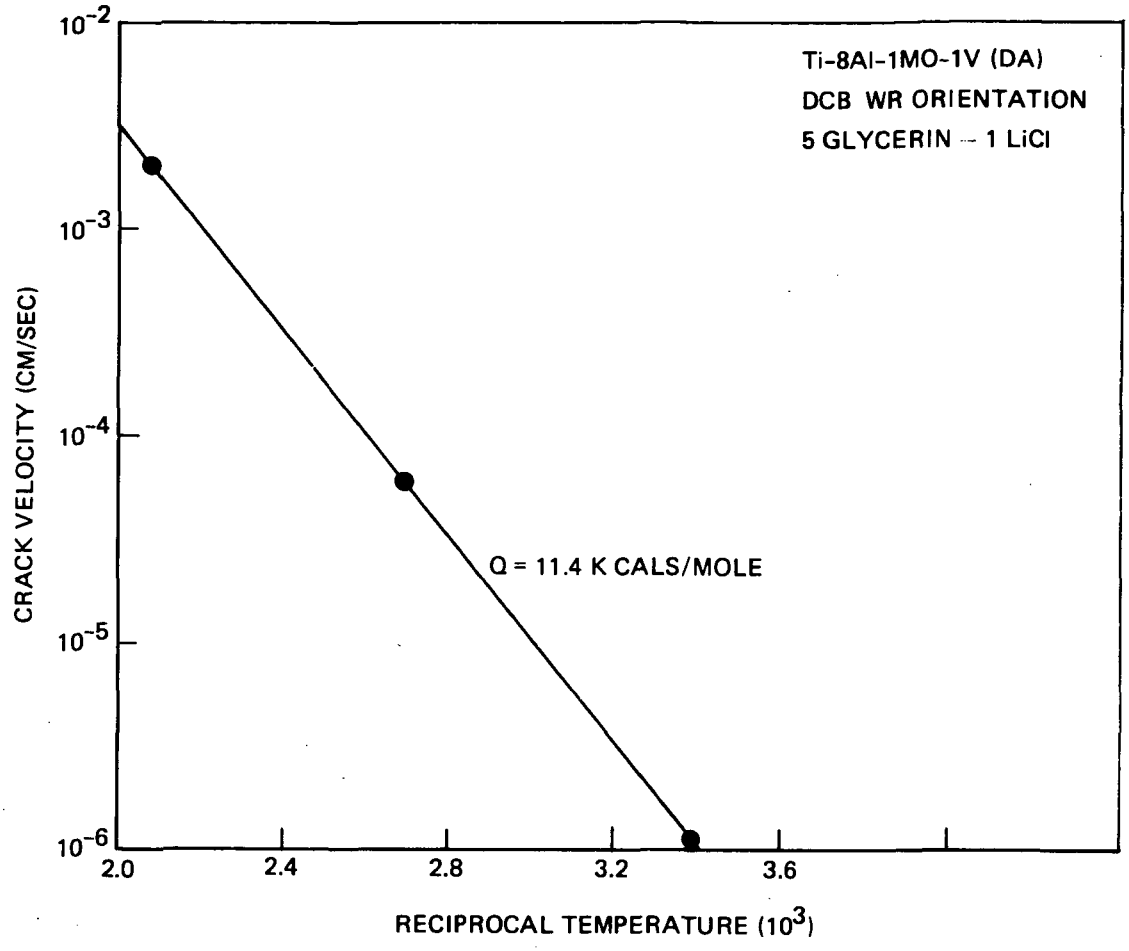

Fig. 5 - (b) The variation of region II (plateau) velocity with reciprocal temperature (°Kelvin) in glycerine: LiCl mixtures. Note the apparent activation energy is ∿12 Kcals/mole.

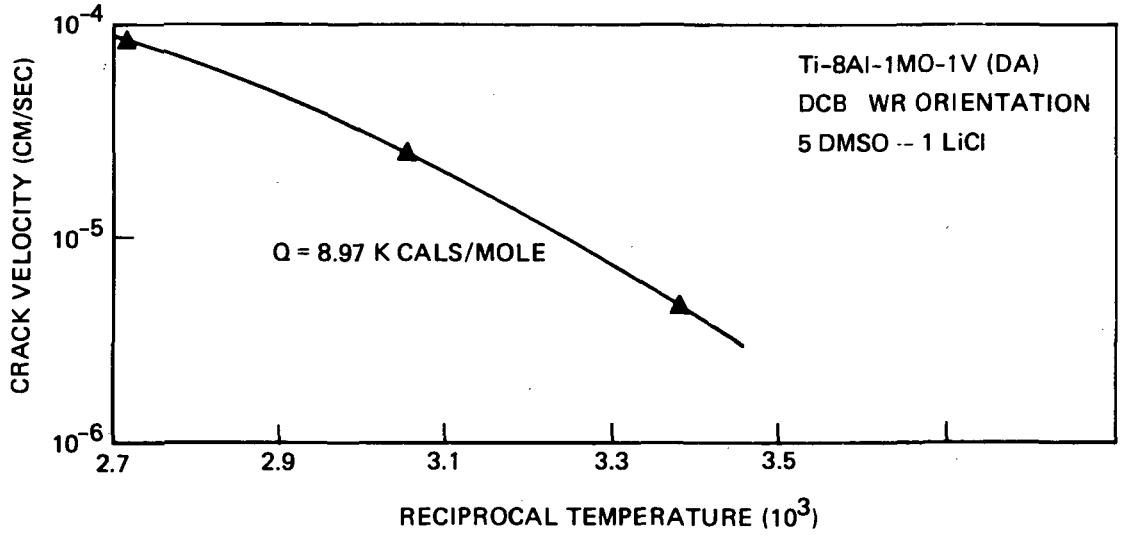

Fig. 5 - (c) Similar results obtained in DMSO:LiCl mixtures which yield an apparent activation energy of ∿9 Kcals/mole.

water - LiCl mixtures which indicates a synergistic effect when comparison is based on viscosity and molarity (but not on an absolute velocity scale).

Supplementary Tests

In this section we note two further groups of experiments that were conducted that certainly influence any interpretation of results but do not fall into any well defined category.

Inert Environments

As mentioned in the introduction results from any group of SCC tests can be complicated by the tendency of a very susceptible alloy to exhibit crack growth in any (and all) environments. The following is a list of aqueous environments in which crack growth was also observed but which did not contain any deliberate additions of the halide ion.

80% sulphuric acid
nitric acid (15.8 M)
saturated $AgNO_3$ ($\sim$10 M).

In all these environments crack growth occurred at rates between 1 and 5×10^{-6} cm/sec. (a complete V:K curve for nitric acid is shown in Figure 11). As cracking was observed to occur at the same rate in dry argon gas such crack growth appears independent of the environment and certainly of its viscosity. Crack growth in any solvent cannot occur at slower rates at room temperature which sets a lower limit on any relationship established (cf. glycerine:LiCl results).

Additions of chloride ions to nitric acid was briefly studied and it was found that crack growth was not accelerated in 3:1 and 2:1 mixtures of 15.8 M HNO_3 and 12.1 m HCl.

The variation in the crack growth in inert environments with temperature was also not studied in detail although such data are of importance in the interpretation of the temperature dependence in more aggressive environments. One test in silicone oil at 100°C showed that cracks propagated slowly (velocity of 10^{-6} cm/sec.) at high K levels (65 ksi$\sqrt{\text{in}}$) which indicates that a low or perhaps negative temperature dependence of cracking in such solutions, and a large increase in K_{ISCC} with temperature.

Influence of Concentration in "Aggressive" Solutions

The data reported in this section is for 5:1 molar ratio mixtures. In the course of this work several tests were run in which the chloride concentration and the cation was varied. It has been shown (14) that in 0.6 M solutions the nature of the cation has little influence on crack growth rate as long as the cation does not influence the potential of the system, e.g., Cu^{++} can lead to low velocities due to the establishment of an anodic potential set by the $Cu^{++} \rightleftarrows Cu^{+} \rightleftarrows Cu$ couples. Tests in which chloride ion concentration was varied with the cation H^{+}, Na^{+}, and Li^{+} indicated that at a constant potential ($\sim$-200 mV):

- In H^{+} solutions, velocity varied as the chloride concentration to the half power;
- In Na^{+} solutions, velocity showed a somewhat low dependence especially in solutions with molarity >1 M;
- In Li^{+} solutions, velocity remained essentially constant at molarities >0.1 M.

However, if the influence of viscosity is considered, these results can be at least qualitatively accounted for since increasing the concentration of solute increases the viscosity most in LiCl and least in HCl. For example, the viscosity of a 9 M LiCl solutions is $\sim$5 centipoise while that of a 9 M HCl solution is 1.8 centipoise.

Also, it may be noted that increasing the concentration of LiCl in glycerine to a mole ration of 1.3 glycerine-1 LiCl produced a solution of higher viscosity than the 5-1 mole ratio solution. The crack velocities in this solution also fall on the glycerine curve as shown in Figure 5(a).

Recapitulation

It was obvious at this stage of the investigation that viscosity provided a good correlation with velocity in one solvent. However, changing the solvent displaced the velocity:viscosity plots and thus viscosity did not provide any overall correlation. Further, the water-glycerine-LiCl results

indicated that any extrapolation from pure solvents to mixed solvents further complicated the relationships. The next logical step it appeared was to look for some factor that was obviously different in the solvents examined and one such possibility was the conductivity of the various solutions. (The reason why conductivity could be expected to lead to differences will be outlined later.)

4.1.3 Velocity-Conductivity Relationships

The conductivity of the test solutions was determined either from existing data or by direct measurement. Next the logarithm of the plateau velocities determined above were plotted against the logarithm of these conductivities with the resulting relationship shown in Figure 6. It can be seen that at least between velocities of 10^{-4} and 10^{-1} a linear relationship is obtained in which velocity varies as the conductivity to the three-halves power. In passing it could be noted that the results for two molten salt mixtures LiCl-KCl at 375°C and NaCl-KCl-$AlCl_3$ at 120°C also lie near but somewhat above the curves for the solvent:chloride mixtures. At velocities $<10^{-4}$ cm/sec. the curves tend to deviate from the linear relationship at least in the aqueous and glycerine solutions. This immediately raises the question why such deviation occur (assuming of course that the relationship observed is not fortuitous). Two possibilities which occurred to the authors were:

- Firstly, reaction products generated within a crack during its propagation produce local modifications of viscosity and conductivity and these changes assume more importance in high viscosity solutions at low temperatures. It is known that the H^+ ion is generated during the propagation of a crack (15) and thus is seemed logical to investigate the viscosity and conductivity of LiCl-HCl-water mixtures at low temperatures. Such solutions were prepared (keeping the $HCl:H_2O$ mole ratio constant at 1:5) and the measurements on the solutions at temperatures as low as -70°C indicated no significant differences from the LiCl:water solutions. This indicated that this hypothesis could not explain the deviation.

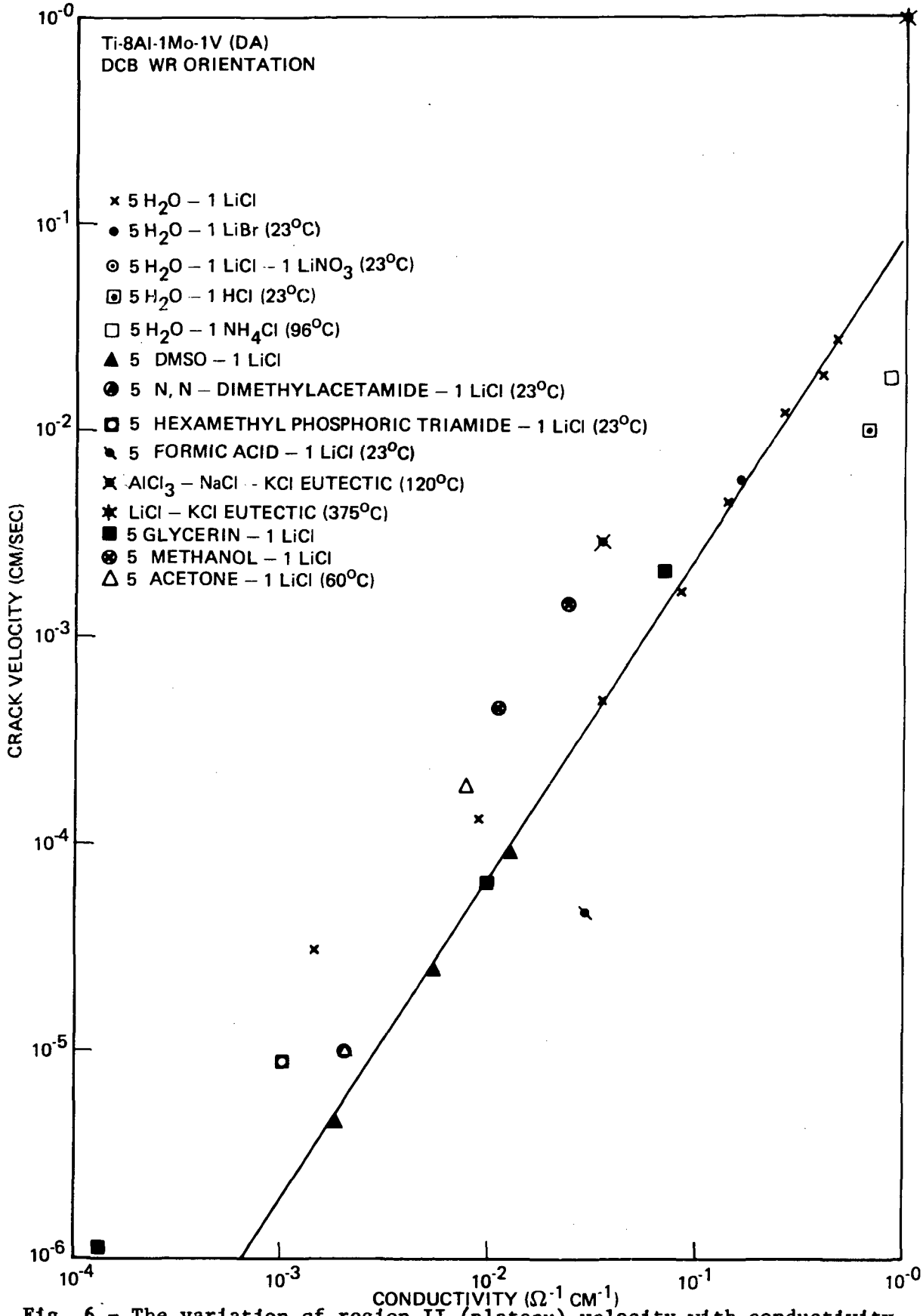

Fig. 6 - The variation of region II (plateau) velocity with conductivity of several solutions containing the halide ions (5:1 mole ratios). Results lie in a scatter band through which a line of slope 1 could be constructed. The line present on this figure is drawn through the LiCl:water and LiCl:DMSO points and has a slope of 3/2. Note that earlier results (Ref. 9) obtained in molten salt mixtures lie near this line.

- Secondly, that potential has a much larger effect at low temperatures and thus open circuit might not be the appropriate potential at which crack velocities should be compared. Measurement of the open circuit potential in the aqueous solution during SCC testing indicated a range of values for open circuit potential of -600 mV $\pm$ 150 mV and that during a specific test the value also varied over about the same range. Thus, a series of tests were performed at fixed potentials at +95°C, +23°C, -25°C and -47°C. These tests were not as detailed as could have been desired due to the number of specimen required and the time involved. At +95°C, cathodic protection still occurs at potentials more negative than -1300 mV but there is little influence of potential in the range -1000 to +1000 mV. At +23°C both anodic crack retardation and cathodic protection are exhibited,* as may be seen in Figure 7. Reducing the test temperature below room temperature results in only minor modifications of the shape of the potential velocity curves. These results indicate that there may be some merit in the suggestion that the basis of comparison may be suspect and-- the conductivity:velocity relationship could be modified considerably by selecting results from several potentials.

---

* The terms anodic and cathodic protection are relative, at cathodic potentials (>1300mV(SCE) cracking rates are reduced to those observed in 'inert' environments. At anodic potentials (>0 mV(SCE) the cracking rates are reduced but in most cases are faster than those in inert environment, thus, in this case anodic crack retardation is probably a better description. It should be noted that such anodic retardation is a strong function of heat treatment and probably preferred orientation, impurity content, etc. of any given alloy. For example, in the alloy studied in this investigation when heat treated to precipitate the α_2 phase within the α phase, which increases SCC susceptibility, essentially eliminates the anodic retardation region at room temperature.

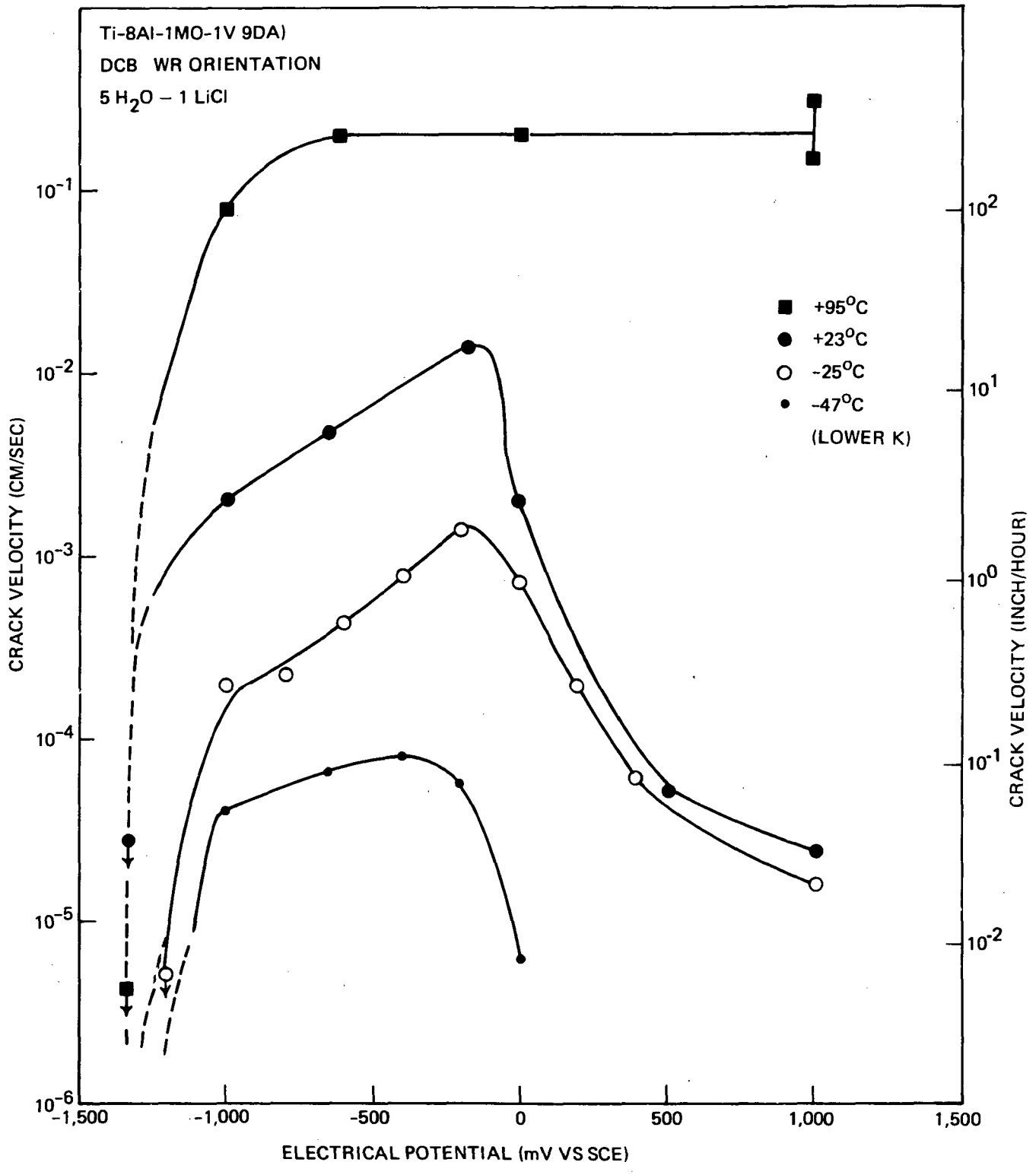

Fig. 7 – The Region II (plateau) velocity vs. potential for Ti-8Al-1Mo-1V measured at several temperatures in 5:1, water:LiCl solutions. Note that cathodic protection occurs at all temperatures but anodic crack retardation does not occur at +96°C although present at lower temperatures.

4.1.4 Potential Studies

Potential Effects in Acid Solutions

Several related series of experiments were performed to check the influence of potential on crack growth in highly acidic environments. Solutions of HCl:water with the same mole ration (i.e., 1:5) were prepared and crack and crack growth measured over a range of potential. The results are shown in Figure 8 in the form of velocity (V) versus stress intensity(K)curves from which it can be seen that as reported previously the region of cathodic protection is eliminated in this solution (16). The plateau velocity shows only a small variation between -1500 and -200 mV and there are indications that the V:K curve at +2000 mV is again similar. However, potentials in the range 0 to +1500 mV again result in rather slow cracking indicating another range of anodic retardation similar to that found in neutral aqueous chloride solutions. There is also evidence indicated in Figure 8 that the velocity is strongly dependent on the test conditions in the anodic retardation region. Results for two tests at +500 mV are recorded, the lower V:K curve is for a test run at potential for the complete test while the results at higher velocity were obtained by switching a crack propagating at -200 mV to +500 mV.(the results from dynamic tests are used in subsequent figures)

The influence of potential on crack growth in 9 M HBr and 5.5 M HI was also studied and the results are shown in Figure 9 . In these solutions there was a more pronounced effect of cathode potentials in that the velocity of cracking was lower at -1000 mV than at -500 mV. However, further reduction of potential led to no further decrease of velocity. Thus in all three acids complete cathodic protection was impossible but the level of plateau (cathodic) velocities is in the order HCl > HBr > HI. (Note that the concentrations of the acids are slightly different.) On the anodic side the behavior in these concentrated acids is more complicated as has been shown previously in neutral solution (14). That is, anodic retardation is observed in chloride and bromide solution while no anodic retardation is found in iodide solutions.

Finally, an attempt was made to extend the passive range in hydrochloric acid, especially to reduce the potential at which hydrogen was evolved to more cathodic values. This was accomplished by adding acetic acid to the HCl

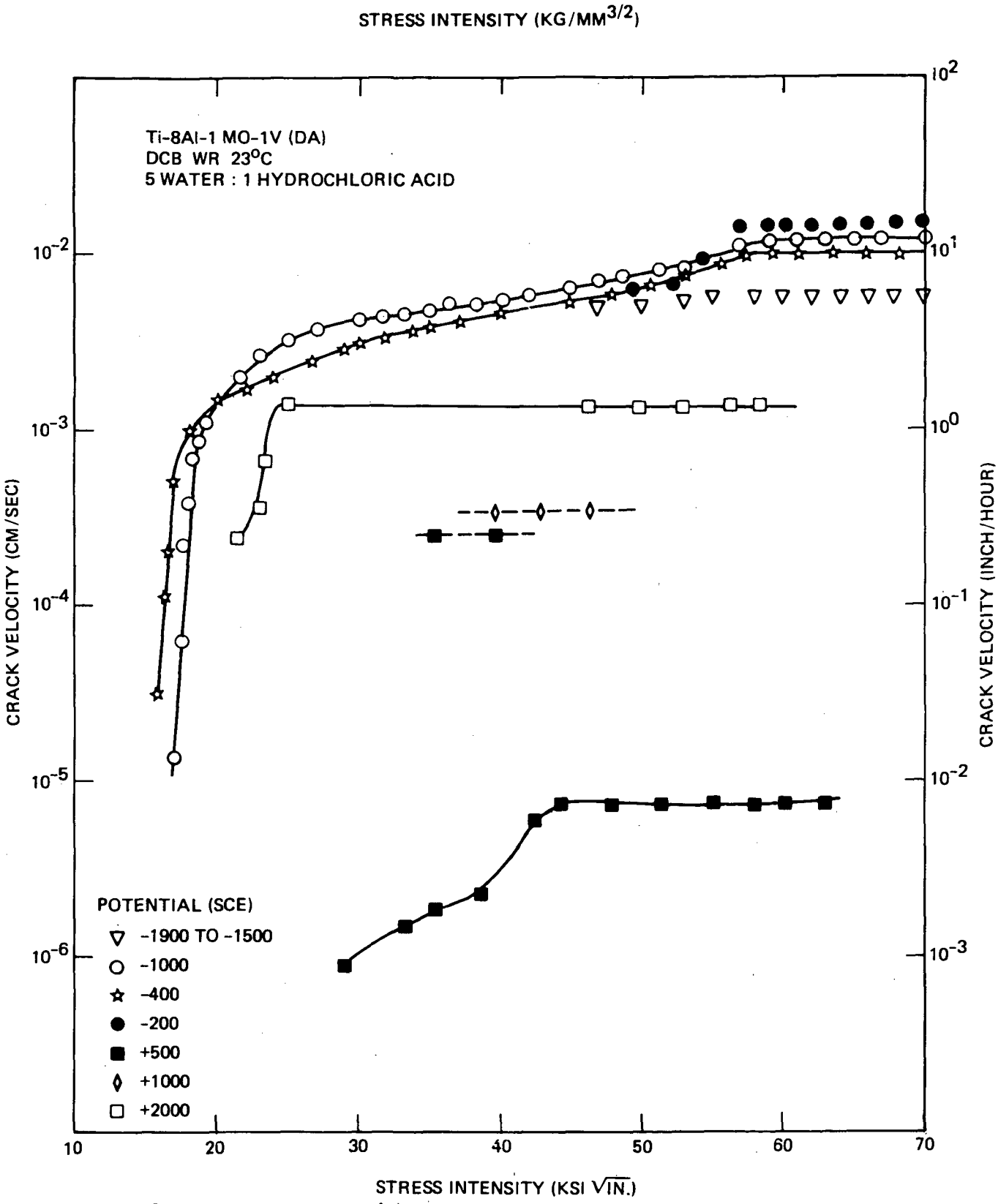

Fig. 8 - Crack velocity (V) vs. stress intensity (K) relationships for Ti-8Al-1Mo-1V tested in 9 M HCl solutions at various potentials at room temperature. The two results for a potential of +500 mV were obrained in a complete test at potential (lower curve) and changing the potential on a dynamic crack at -200 mV (upper points).

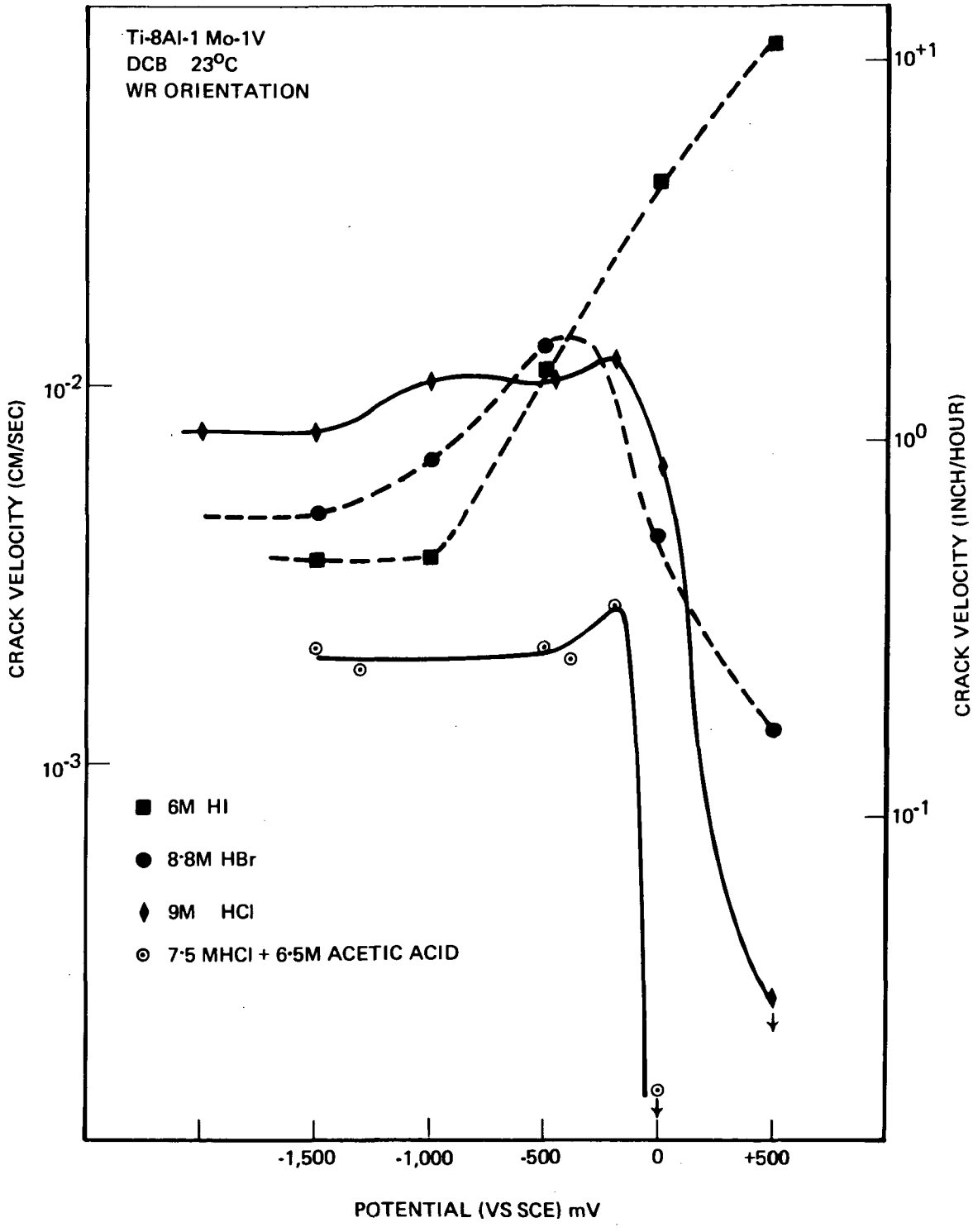

Fig. 9 - Region II (plateau) velocity variation with potential in three concentrated halegon acid solution at room temperature. Note that cathodic protection does not occur in such solution and that anodic potentials produce more complicated behaviors.

which reduced the potential for copious hydrogen gas evolution (controlled by the iR drop) on an oxide covered specimen from ∿-400 mV to ∿-800 mV. The results shown in Figure 9 illustrate that the velocity of crack propagation is reduced in such solution mixtures but the general potential: velocity results parallel the results in hydrochloric acid.

From these and additional tests (17), it appeared that the influence of potential on crack growth is strongly temperature dependent which if nothing more complicates the establishment of any relationship involving velocity determination at open circuit potential. It is of interest that the influence of potential decreases at elevated temperatures which is parallel to the behavior observed in molten salt solutions where again the plateau velocities are independent of the applied potential (8).

Potential and pH

It had been suggested previously by proponents of both the anodic dissolution (18) and hydrogen embrittlement (19) postulates for the mechanism of SCC in aqueous solutions that the essential reason for cathodic protection is that OH^- ions are generated at the crack tip. The arguments on the influence of such OH^- ions on crack propagation are obviously slightly different for the two cases but the details need not concern us here. To study solutions with high pH and coupled high concentration of halide ion is rather difficult due to the relatively low solubility of the hydroxide in the case of lithium and the low solubility of the chloride in the case of sodium and potassium. Thus we used a compromise solution containing 3.5 M sodium chloride and 3.5 M sodium hydroxide. The influence of potential on crack velocity in this solution is shown in Figure 10 compared with those observed in acidic and neutral solutions. It can be seen that the behavior is very similar to that in neutral solution. However, the region of cathodic protection is shifted from potentials more negative than -1300 mV (neutral) to more negative than -900 mV (basic).

Addition of Ti^{3+} Ions

It has been proposed that dissolution of titanium is the critical step or at least forms part of the process of SCC (20). The titanium species

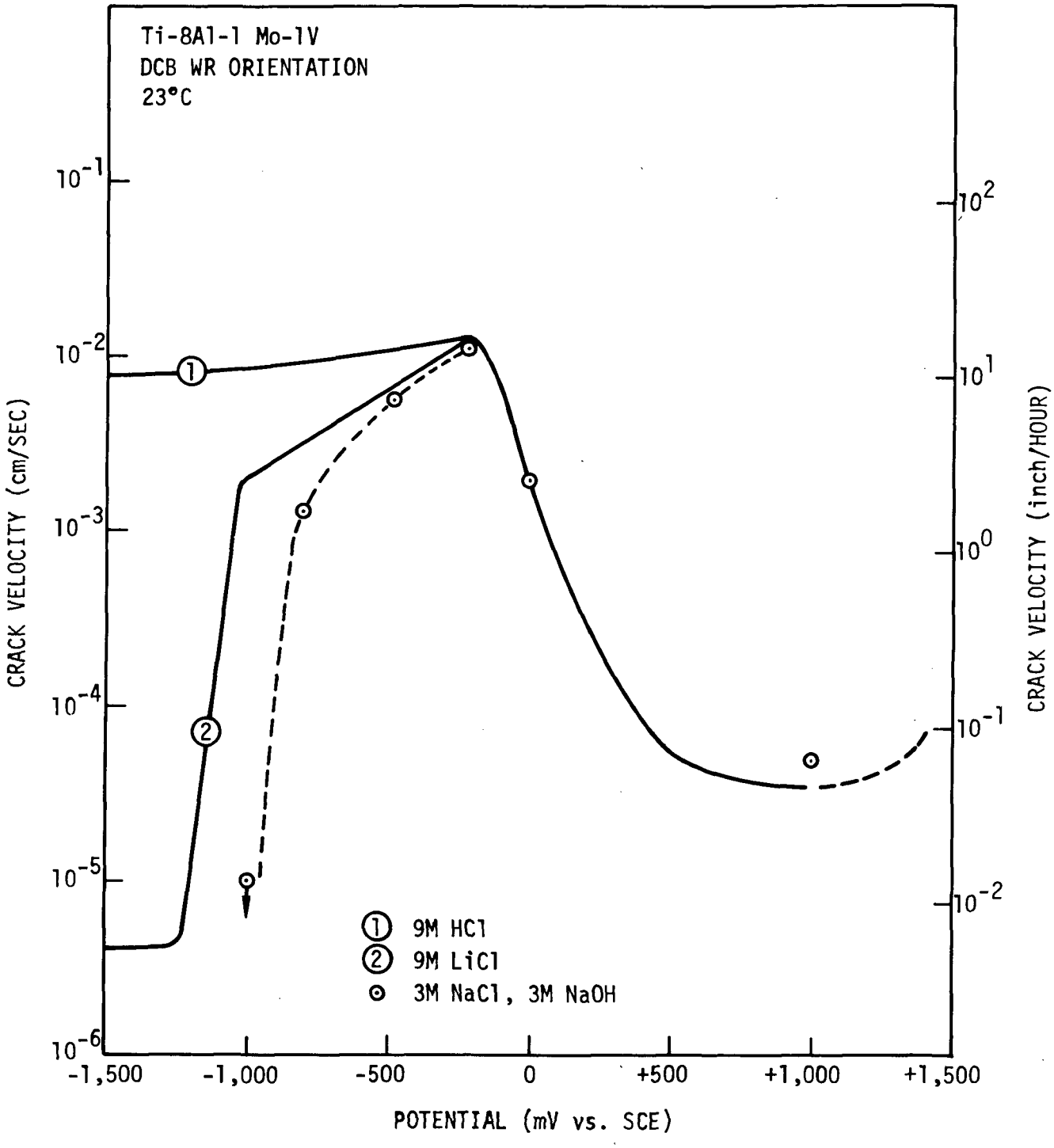

Fig. 10 - Variation of region II plateau velocity with potential in acidic (Figure 10) neutral (Figure 8) and basic solutions. Note the similarity of maximum velocities at -200 mV and that anodic crack retardation is observed in all solutions. Cathodic protection does not occur in the acid solution but is present in neutral and basic solutions.

that forms in acid solutions (pH=0) at potentials between -800 and 0 mV should be Ti^{3+} and thus it was considered that the presence of this ion in solution could influence SCC behavior. The Ti^{3+} ion is unstable in neutral aqueous solutions and thus an acidic solution was utilized, specifically a solution of 9 M HCl saturated with $TiCl_3$. (The solubility of $TiCl_3$ in the solution is high, >1 M in 9 M HCl.) A test was performed in this solution at open circuit (-350 mV) and the resultant V versus K curve is shown in Figure 11. Comparison of this result with the V:K curve for 9 M HCl at -400 mV (Figure 8) indicates the two curves are identical below a K value of 42 ksi$\sqrt{in}$. The plateau velocity in the HCl:$TiCl_3$ solution was slightly lower than that in the HCl solution. One final point of interest is that a strongly stress intensity dependent crack growth (Region I type growth) is observed in concentrated HCl solutions at low K levels appeared to be eliminated in the $TiCl_3$:HCl solutions, as crack growth did not occur below a velocity of 10^{-4} cm/sec.

4.1.5 Solutions Containing Non-Ionic Chloride

A reasonably logical extension of these tests in liquid environments containing the chloride ion appeared to be a study of solutions which contain chloride in other forms. It had been established that some titanium alloys are very susceptible to stress corrosion cracking in carbon tetrachloride (CCl_4). In order to see if the crack velocity in this solution varied with temperature (and thus viscosity) three tests were performed over the temperature range +50 to -25°C. These results indicated that in this solution the crack velocity does not depend on viscosity in any simple way. The approximate apparent activation energies determined from these SCC tests were ∿4 Kcals/mole above room temperature and ∿9 Kcals/mole below room temperature.

Two further tests were conducted in chloroform ($CHCl_3$) in order to evaluate the influence (if any) of replacing one -Cl by -H in the solvent. Both tests indicated that initially the crack grew at very slow rates, $\sim 10^{-6}$ cm/sec. but after induction times varying from 8-70 hours the cracking accelerated and reached comparable values with those observed in CCl_4.

Finally one test was performed in titanium tetrachloride ($TiCl_4$) which yielded the velocity stress intensity curve shown in Figure 11. The velocity of

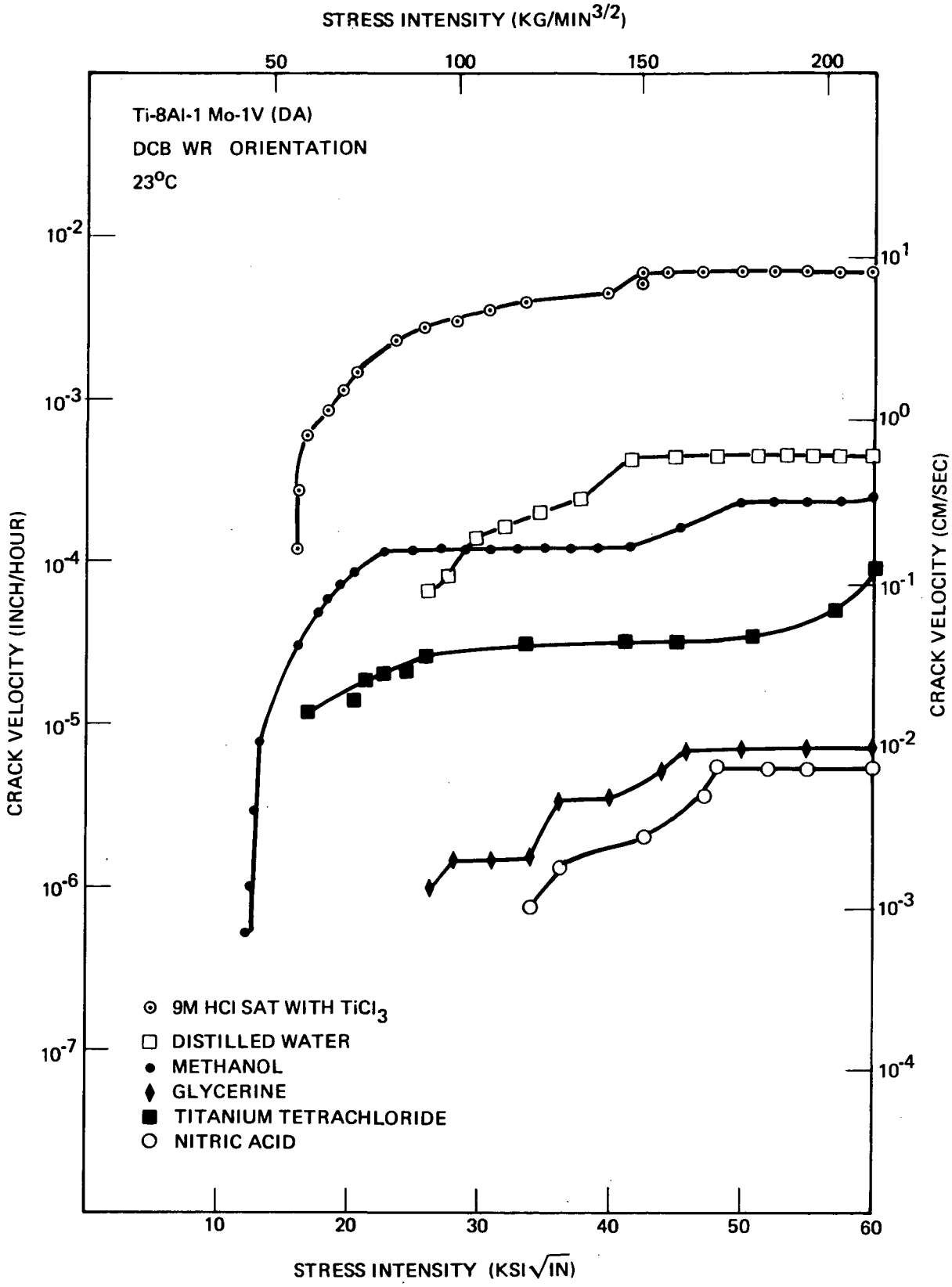

Fig. 11 - Crack velocity (V) vs. stress intensity (K) for Ti-8Al-1Mo-1V tested in several solutions. Note the similarity of the HCl:$TiCl_3$:water curve with the -400 mV curve in Figure 9, with the exception of region I type crack growth. The velocity results in titanium tetrachloride are very similar to cracking rates observed in DMSO:LiCl type solutions (Figure 6a) and in the anodic crack retardation range (Figures 8-11).

cracking was relatively slow in this solution yielding a plateau velocity of $\sim 7 \times 10^{-5}$ cm/sec. coupled with a low K_{1SCC} level. However, the existence of Region I behavior could not be excluded on the basis of one test.

4.1.6 The Value of K_{1SCC}

For completeness the values of K_{1SCC} determined in the above tests are listed in Table I. It should be noted that Region I type behavior was found in some solutions which are marked with an asterisk(*) and the value of K_{1SCC} is quoted for a crack velocity of 10^{-5} cm/sec. As there is no really quantitative explanation of the value of K_{1SCC} at this time (1) the table is presented with no further comment.

(i) PURE SOLVENTS

SOLVENT	WATER	METHANOL	GLYCERIN	CARBON TETRACHLORIDE	CHLOROFORM
K_{1SCC} (Ksi$\sqrt{in}$)	26 (23)	13.8 (23)*	26 (23)	19.4 (-11)	21 (23)
and				20 (23)	
(Temperature °C)	42 (96)			19.5 (50)	

(ii) SOLUTIONS CONTAINING CHLORIDE OR BROMIDE IONS, 5:1 SOLVENT: SOLUTE RATIO

(a) Open Circuit

SOLVENT / SOLUTE	WATER LiCl	METHANOL LiCl	GLYCERINE LiCl	DMSO LiCl
K_{1SCC}, Ksi$\sqrt{in}$	>20 (-46)	13 (23)*	19 (23)	19 (23)
(Temperature °C)	22.7 (-26)		26 (96)	>25 (55)
	20.3 (-3)	13 (58)*		
	17.0 (+2)		26 (210)	
	14.7 (23)			
	21.8 (60)			
	20.8 (96)			
	22.7 (113)			

(b) Open circuit, room temperature, 23°C

Hexamethylphosphoric Triamide	27.8
N,N-Dimethylacetamide	30.6
Water-Lithium Bromide	19.5

(c) Open Circuit - other temperatures (°C)

Acetone-Lithium Bromide	>30 (66)
Water-Ammonium Chloride	26 (95)

(iii) MIXED SOLVENTS CONTAINING CHLORIDE IONS; 5:1 SOLVENT-SOLUTE RATIO, OPEN CIRCUIT (ROOM TEMPERATURE 23°C)

Eormic acid, water, Lithium Chloride	25 (23)
Water, HCl, 1 M $TiCl_3$	16.3 (23)
Water, 9 M $LiNO_3$, 9 M Lithium Chloride	23.2 (23)
Water (3.4), DMSO (1.6), Lithium Chloride	19.5 (23)
Water (4), Glycerine (1), Lithium Chloride	19 (23)
Water (2.5), Glycerine (2.5), Lithium Chloride	18 (23)
Water (1), Glycerine (4), Lithium Chloride	24.5 (23)

(iv) SOLUTIONS CONTAINING CHLORIDE IONS, 5:1, SOLVENT:SOLUTE RATIO VARIOUS TEMPERATURES AND POTENTIALS (mV vs SCE)

SOLUTION	TEMP °C	(POTENTIAL VS SCE)			
Water:LiCl	23°C	23.2 (-1000)	19.9 (-200)		20 (+20000)
	95°C	29 (-1000)	22.2 (0)	21.3 (+10000)	23.9 (+2000)
Water:HCl	23°C	17*(-1000)	15.5*(-200)	27.7 (+500)	20.8 (+2000)

(v) MISCELANEOUS

Water, 0.1 M Lithium Chloride, Open Circuit	23.1 (2), 24.8 (23), 30.2(90)
Water, 0.6 M Sodium Chloride (-500 mV)	20 (23)
Water, 3.5 M NaCH, 3.5 M Sodium Chloride	21.4 (23)

(vi) INERT ENVIRONMENTS

Room Temperature	- 36-45
100°C (Silicone Oil)	∿65

4.1.7 DISCUSSION

The essential points established by the experimental work described above are that Region II or plateau velocities can be correlated with the viscosity and conductivity of the solution. This discussion is divided into three parts in which we examine possible influences of these physical properties on processes that could occur in stress corrosion cracks. Anticipating the result of these speculations we shall conclude that no simple explanation for a rate controlling process is possible and thus add a fourth section on a more detailed analysis of chemical factors that contribute to cracking. It should be noted at this point that several factors recur in the following paragraphs as follows:

- There is an implicit assumption that the basic process that controls the rate of crack extention is (more or less) the same in all the environments studied;
- In many cases chemical reactions that occur in cracks are assumed. It can be noted in passing that the chemical conditions in cracks are certainly not well defined. Further, controversy exists on the basic thermodynamic equilibrium in the titanium-water system (21,22) and the study of the kinetics of these reactions is still in its infancy;
- Reference will be made to the so-called theories of stress corrosion cracking which fall into three groups, hydrogen embrittlement, dissolution and adsorbtion processes. We shall not be concerned with providing a critical evaluation of these theories but to examine if their rather vague formulations are in any way consistent with our results.

Fluid Flow

The fluid flow characteristics in a propagating crack have not received much attention in the past. Some attempts have been made to treat the hydrodynamics in liquid metal embrittlement (23), but have employed models which are not generally useful. The problem is of importance for two reasons: (i) the fluid flow could limit the velocity of cracking, by the onset of

"cavitation" in the crack, and; (ii) even if cavitation is not important in limiting the crack propagation, the fluid flow characteristics may be important in determining concentration distributions in a crack where mass transfer is critical to crack extension (see next Section).

For a wedge-shaped crack propagating through a material immersed in a liquid, the hydrodynamics may be shown (24) to depend on the crack geometry, the physical properties of the fluid, the total pressure drop down the crack, and the velocity of crack propagation. In the outer part of the crack, inertial and pressure forces are predominant, but nearer the crack tip only viscous and pressure forces are important. The viscous shear stress increases as one approaches the crack tip, creating a pressure drop. If the shear stress becomes large enough, the pressure could be lowered enough to produce a "cavity" of vapor. This would interrupt the fluid flow, decreasing the crack velocity until a balance could be attained between the velocity of crack propagation and the tendency to form a cavity, and thus a maximum steady-state velocity of cracking. The velocity would be expected to be inversely proportional to the viscosity for a constant crack geometry and pressure drop.

The results for an individual system in Figure 5(a) reveals that the velocity of Region II cracking indeed is inversely proportional to the viscosity. However, the different systems are displaced (parallel) with respect to one another. This indicates that the absolute value of the viscosity is not controlling the absolute velocity of cracking for all these systems. The water, methanol, and glycerin data could probably be made to coincide at one temperature by accounting for differences in crack geometry and vapor pressure, but the dimethyl sulfoxide and acetone data are too low (on a velocity basis) to be "corrected" in this way.

One effect of temperature on the liquid would be to increase its vapor pressure. This should lead to a lower velocity at higher temperature, if the cavitation phenomenon determines the plateau velocity, for it should facilitate cavity formation. This could be compensated to some extent by the reduction of viscosity at higher temperatures which would tend to allow higher crack velocities. From the data in Figure 5(a) there is no indication that the vapor pressure change for the indivisual liquids influences the

limiting velocity of a crack. Since data were taken near the boiling point for the methanol and water solutions, some effect of vapor pressure should have been found there if cavitation was the rate controlling step.

We have assumed that cavitation would occur when the pressure in the liquid drops below its vapor pressure. It is known that vapor bubbles are hard to nucleate in narrow passages (25) with the result that one may not observe cavitation until very "negative" pressures are attained. The properties of liquids under such tensile loads have been measured (26), and the ultimate tensile strength of a van der Waals liquids have been calculated (26). The ultimate tensile strength decreases with temperature, again leading one to predict a decrease of velocity with increasing temperature.

The description of fluid flow characteristics used here (24) has been for the case where there is no transfer (dissolution) of the solid into the liquid. If there were dissolution, it could influence the fluid flow so that cavitation would occur below a certain velocity for a given rate of dissolution. Dissolution would act to decrease the viscous shear stress and thus to decrease the pressure drop in the crack. We conclude therefore, that fluid flow cavitation does not control Region II velocities in these systems as the separate curves obtained coupled with the lack of vapor pressure or strength effects near the boiling point indicate a more complex phenomenon. The effects of "negative" pressures and of dissolution may be of importance in situations (i.e., near the boiling point) where the greatest influence of cavitation would be expected to occur. The interrelation between fluid flow and mass transfer (e.g., dissolution) will be discussed more fully in the following section.

Convective Diffusion (Mass Transfer)

In the first part of this section it will be assumed that the viscosity of the solution controls the rate of stress corrosion crack propagation by influencing the rate of mass transfer. The kinetics of some electrochemical reactions can be controlled by such transfer rates, an example being the deposition of copper under certain conditions. Diffusion will occur as the result of a nonuniform concentration distribution and convective flow usually determines the distances over which the concentration changes. A

simple example is the rate of dissolution of a solid salt into a solution which does not contain the salt which may be expressed approximately by the equation

$$J = \frac{Dc}{\delta}$$

where D is the diffusion coefficient of the salt
C is the concentration of the salt
δ is the diffusion layer thickness.

The viscosity of the solution can influence the rate of reaction in two ways:

- The diffusion coefficients of salts are changed by the viscosity and for many systems may be expressed by the empirical correlation

$$D \propto \frac{T}{\eta}$$

where T is the absolute temperature and
η is the viscosity

- The diffusion layer thickness δ is also influenced by the viscosity and by the prevailing hydrodynamic conditions. For flow past a flat plate and flow to a rotating disk, δ varies as the one sixth power of the viscosity.

It is therefore concluded that the influence of viscosity on a mass transfer controlled SCC reaction will be predominately through changes in diffusion coefficients.

Returning now to the assumption that the velocity of cracking is controlled by a mass transfer limited chemical reaction, it is obvious that our results are consistent with this hypothesis. The linear viscosity: velocity relationships shown in Figure 5(a) also shows three separate curves are obtained for the individual solvents. Plotting the results as log V vs log $(\frac{T}{\eta})$ changes the pattern very slightly, making the slopes more nearly unity but leaving separate curves for different solvents. This in turn could be consistent

if the absolute values of the diffusion coefficients were different for the various solvents. As may have been predicted, data on diffusion coefficients are not available. However using the values for infinite dilution (a situation far removed from these solutions) one would predict that as the diffusion coefficients fall in the order

$$H_2O > MeOH > DMSO$$

that the SCC velocities would fall in the same order which indeed they do. Unfortunately, the absolute values do not correspond to the relative displacement of the curves especially in the case of the DMSO solutions

Having shown a general correlation it is pertinent to examine which processes in a stress corrosion crack could be mass transport limited, and more specifically consider the species that may be involved in the rate limiting step. For the systems investigated, it is considered that the solvent molecules may be excluded due their high concentrations which leaves--

- The Li^+ ion
- The H^+ ion derived from the solvent or some chemical reaction
- The Cl^- ion
- The Ti^{3+} ion derived from a chemical reaction
- The $(TiO)^{2+}$ ion

The alkali metal cation derived from a chemical reaction is not likely to be important in a diffusion limited process as it is not consumed by raction that could occur. Further it has been shown (14) that the nature of the cation does not have a marked influence on SCC rates.

The hydrogen ion is a more serious candidate as it has been suggested that SCC in titanium alloys is related to a hydrogen embrittlement process (19). The rate of reduction of hydrogen ions in aqueous solutions could be quite large under diffusion-limited conditions. However, hydrogen gas bubbles would begin to form at much lower currents than this limit tending to block the surface and reduce the reaction rate. This would prevent one from

observing a current limited by hydrogen ion diffusion. However, blocking the surface by a gas bubble would impose a limit on the amount of hydrogen ion reduction which could take place. The rate of diffusion of dissolved hydrogen (into the metal, or into the solution) would be balanced by the rate of production of hydrogen by hydrogen ion reduction. This general idea is not new, and has been discussed elsewhere (27)(for a discussion of gas bubbles blocking an electrode in another application, see Ref. (28)). This does not appear to be a likely process for controlling cracking in all our studies for the following reasons:

- There should have been no influence of (cathodic) potential on crack velocity;
- There should have been no cathodic protection;
- It conflicts with trend of solubility of hydrogen as a function of temperature and solvent;
- Hydrogen is probably not generated in the DMSO and other solutions.

The chloride ion could be involved in a mass transfer limited reaction in two ways:

- Oxidation to Cl_2 gas, which is unlikely as cracks may propagate at potentials far removed from that required for the formation of chlorine gas;
- The formation of a solid chloride film ($TiCl_3$) or the formation of a titanium ion complex. Discussion will be restricted to the former case although the arguments based on complex formation would be similar.

This latter suggestion could also be considered to be relevant to the process of crack extension, which may occur by a (selective) dissolution mechanism. The limiting step in such a dissolution process could involve the formation of a solid film of $TiCl_3$ (20) on the crack surface, and the diffusion of the salt from this surface. This diffusion rate would depend on the concentration of $TiCl_3$ at the interface (determined by solubility) and the magnitude of the total anodic current would be an inverse function of the chloride ion concentration. Such a process also involves the diffusion of Ti^{3+} ions and

indicates one way in which these ions could be involved in a mass-transfer limited process.

However, limiting the cracking rate by an anodic dissolution process controlled by solid solubility is inconsistent with our results in the following ways:

- The influence of temperature on cracking rates reflected only changes in viscosity. Thus, the solubility of the salt would have to be temperature invariant to be consistent with the results;
- Cracking rates should be inversely proportional to chloride ion concentration due to the influence on solubility. This is inconsistent with earlier results (1) and some data reported here.
- Saturating the bulk solution with $TiCl_3$ should have decreased or even stopped cracking which it did not (see Fig. 11).

If no solid film is formed to control the process, dissolution will probably be controlled by ohmic and/or kinetic factors. Again such processes could well be complicated by film formation such as oxides.

The fourth possibility, the Ti^{3+} ion, for a mass transfer limited reaction also involves a dissolution step. For example, if Ti^{3+} were formed at the crack tip and oxidized to a four valent species at some distance from the crack tip the process could be limited by the diffusion of the Ti^{3+} ion to the oxidation position. As the distribution of the oxidation reaction along the crack wall is the current distribution it will determine the potential drop within the crack. This potential distribution will be of importance in setting the potential at the crack tip with respect to the external potential and thus will determine the anodic dissolution rate. The total potential drop would be proportional to the conductivity of the solution, and this is another way conductivity might be important to crack extension rates. Thus, if dissolution controls the rate of crack advance overall control would be exercised by the diffusion limited oxidation rate along the crack wall. It should be noted that a similar argument could be constructed

if the reduction of the Ti^{3+} ion was possible in these solutions. Controlling the cracking rate through a mass transfer limited reactions of titanium ions on the crack walls appears unlikely for the following reasons:

- The only stable species in aqueous (and methanolic) solutions are Ti^{3+} and (TiO^{2+}) (in alcoholic solutions, the four valent species is probably an alcoxy-chloride complex (29)). It is improbable that potentials within the crack deviate from the applied potential sufficiently to allow the oxidation or reduction of these species for the range of potential over which cracking is observed. For example potentials of 0 to +200 mV would be required to oxidize Ti^{3+} to (TiO^{2+}) and cracking occurs in neutral solutions at -1000 mV. (See Fig. 8).
- In several solution such as DMSO, formic acid, N-N dimethyl-acetamide, etc. only one species of titanium is stable, (TiO^{2+}) (or a compound similar to the methny species formed in methanol), which can neither be oxidized nor reduced. The solvent is reduced more easily than four valent titanium.

Thus we may conlude that a simple mass-transfer limited process cannot be rationalized as the limiting process for SCC in these solutions at present. In many chemical reactions at current levels lower but at appreciable fractions of the mass-transfer limited current, kinetic and ohmic contributions can be substantial. Diffusion effects may still be contributed and be sensitive to viscosity, stirring etc. Therefore, although we find none of the above processes to control cracking, they could make a contribution to overall control. It may prove that a more complex model is appropriate but at present insufficient data exists to aid in its formulation. The model due to Beck and Grens (30) may indicate the direction in which such a formulation should take but in its present form is probably an oversimplification of the processes occurring in SCC.

Conductivity

It was shown in the experimental results section that there was a reasonably good correlation of crack velocity with the bulk conductivity of the solution. For a chemical reaction which is under ohmic control the

conductivity determines the level and distribution of current for a given overpotential. This primary current distribution is such that the smallest current flows to the points of the electrode most distant from the counter electrode. For an electrode with a wedge shaped crevice it can be shown that zero current would flow to the tip. Thus is is doubtful that reactions giving a primary current distribution could contribute to crack extension. However, if the kinetics of a reaction are important the primary current distribution can be moderated, i.e., made more uniform. Of special relevance are the influence of surface films such as oxides which change kinetics dramatically and thus dominate the electrochemical properties of many metals. Such passivation effects level the current distribution making it possible to conduct current into a crack and probably to the crack tip.

There is considerable evidence that the walls of an advancing SCC crack are passive which results in a relatively small potential drop down a crack (in most situations). For example, reaction products (which depend on the solution and potential) such as hydrogen, $(TiO^{2+})_x$ and iodine are observed to form near the crack tip at least at the intersection of the crack with the external surfaces of a specimen. These observations have been confirmed more directly by propagating a crack in a specimen in a neutral iodide solution at a potential (+500 mV) at which iodine was liberated. The crack was arrested by rapid immersion of the specimen in liquid nitrogen and subsequently broken open at low temperatures. Visual and microscopic (10 X) observation showed that iodine, confirmed using a starch indicator, was present to the stress corrosion crack tip. Thus, it is concluded that there is only a small potential drop down a propagating crack at least in neutral solutions. This appears to be consistent with the ohmic drop measured when SCC tests under potential control were open circuited (20), also, the Beck-Grens model was unable to account for any large potential drop down a crack. Thus, if the tip of a crack is more active than the walls, current may go preferentially to the tip region and thus result in greater control of a reaction in this region by any externally applied potential. If the current flowing to a specimen is small in the absence of cracking then the current flow during cracking may be indicative of reactions occurring at the crack tip. In experiments in neutral solutions at potentials between -800 mV

and 0 mV where the background current is low it has been demonstrated (14) that an anodic current is produced during cracking, indicative of an overall anodic reaction. This is a net current however, and both anodic and cathodic processes may be occurring within the crack.

Thus, with the assumption that the crack tip is sensitive to the applied potential we may examine the possibility that crack tip reactions are ohmically controlled. It could be predicted that the crack velocity should be proportional to the conductivity for a constant potential drop or proportional to the potential drop for a constant conductivity, both types of data are reported in the experimental section. Figure 6 includes the stress corrosion crack velocity and conductivity for LiCl-H_2O solutions as a function of temperature. At high temperatures the relationship is linear but the points tend to deviate at lower temperatures. The high temperature results lie on a line of slope 1.5 which is greater than the slope of one expected for simple ohmic control for a reaction. It should be noted that the data in Figure 6 was taken at open circuit and this may not represent a constant overpotential for the reaction. Measurement of the open circuit potential with respect to a room temperature calomel electrode showed that this remained relatively constant with temperature at-600 mV ($\pm$100 mV). However, as the potential dependence for the rate of crack growth varies with temperature the exact meaning of the open circuit potential is not clear. The influence of potential and temperature on crack velocity is shown in Figure 7 which reveals that

- Cathodic protection is observed at all temperatures;
- Anodic protection (or more exactly crack retardation) is observed only at low temperatures.

The data in Figure 6 is taken at potentials which are near the peak velocity for all the temperatures studied but as the potential dependence is temperature dependent the constant overpotential assumption is suspect. We defer discussion of the regions of anodic and cathodic protection to the section on Chemical Effects.

Turning now briefly to the behavior in the other solvents, the results in glycerine and methanol lie close to the results for water solution with

the glycerine results agian deviating at low temperatures. In both solutions the open circuit potentials were ∿-500 mV and cathodic protection was possible at -1500 mV. The DMSO results lie on the extrapolation of a line drawn through the high temperature water-LiCl points. In these solutions the open circuit potential was ∿-200 mV and there was little influence of potential although at high temperatures (96°C) there was some evidence of cathodic protection. In the other solutions, tests were only conducted at ambient temperatures (23°C).

The correlation between SCC velocity and conductivity of all solutions tested is surprisingly good-- in fact, a line with a slope of 1 could be constructed through the scatter and the conclusion that SCC occurs by an ohmically controlled chemical reaction would seem quite convincing. However this implies that

- the same reaction occurs in all solvents-- which is most unlikely (see Chemical Effects Section);
- the reaction occurs at a constant overpotential;
- the effect of concentration (of Cl^-, Br^- of I^-) could be accounted for by their influence on the conductivity of the solution.

In connection with this last point it should be emphasized that we have only considered crack growth in solutions with 5:1 mole ratios of solvent: salt. Changing the concentration of the Cl^- ion produces large deviations from the velocity-conductivity relationship established in these solutions as illustrated semischematically in Figure 12, which shows that the points lie above the curve. It is possible (but not proven) that points below the curve could be obtained by mixing chloride with high conductivity "inhibitors" such as nitric or sulphuric acid. A final point on mixing solutions is that deviations can also be produced by mixing solvents at a constant chloride ratio. This is illustrated in Figure 7 for water-glycerine-LiCl mixtures. None of these observations support the ohmically controlled reaction hypothesis.

Thus we must again conclude that although the evidence is at first sight suggestive, the controlling step in the propagation of cracks in these solutions cannot be simply accounted for by a chemical reaction under ohmic control.

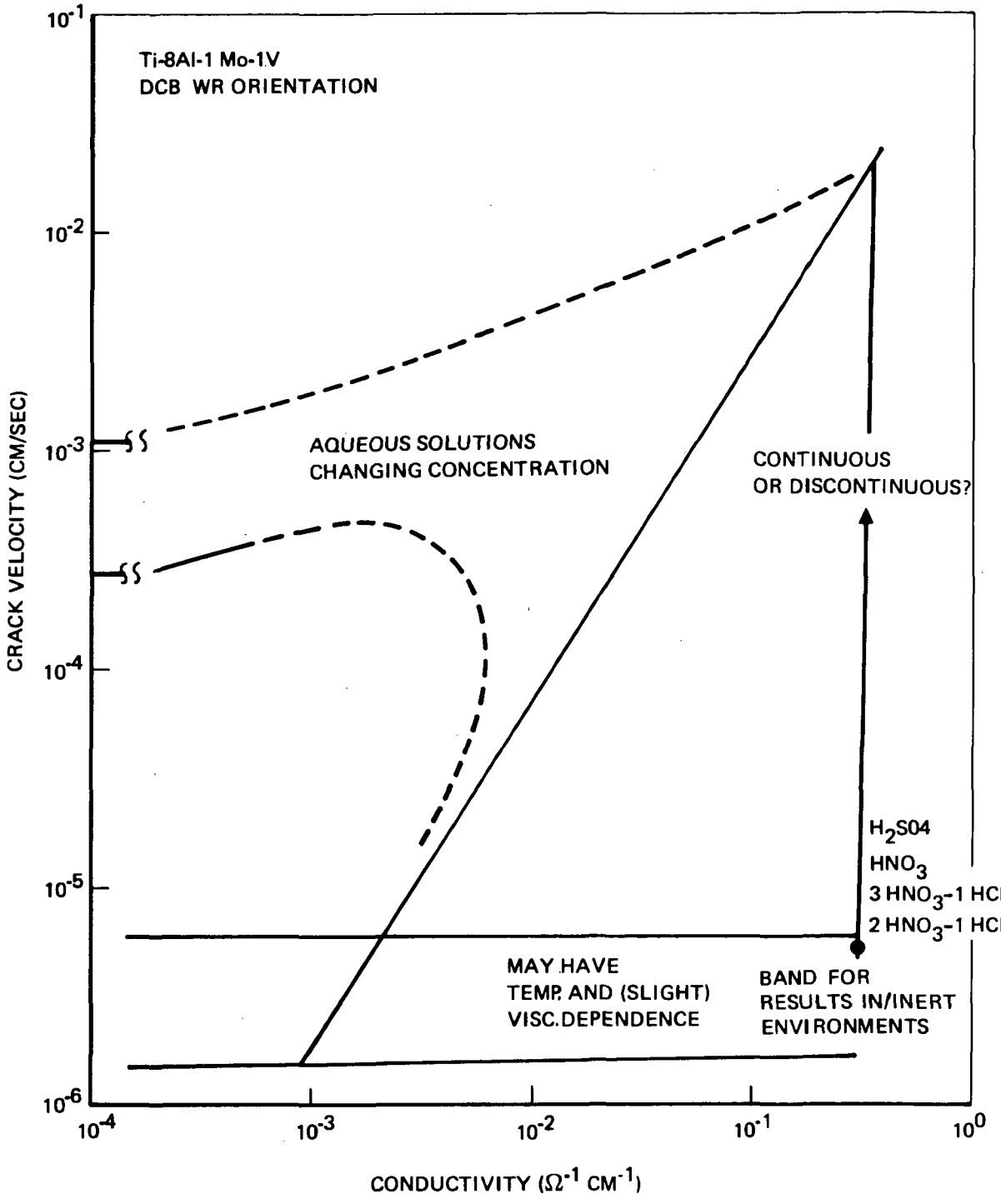

Fig. 12 Semischematic diagram of the changes in the velocity: conductivity relationship (Fig. 6) produced by varying the halide ion concentration. Reducing this concentration in aqueous (and other solutions) produces points above the line for the 5:1 mole ratio solutions. It may be possible to produce points below the line by the addition of halide ions to high conductivity inhibitor solutions (eg HNO_3, H_2SO_4, etc).

Chemical Factors Influencing Crack Propagation

At this stage we have reached the unsatisfactory state of having established rather attractive experimental correlations and provided at least three superficially logical explanations, most of the discussion had been concerned with demolishing these explanations. This again leads to the conclusion that any elementary explanation of SCC is unlikely. In this section we shall deal with selected aspects of the chemical part of the problem emphasizing some of the more positive points and correlations that have been established in this work.

Velocity-Viscosity Correlation

It was noted earlier that in Figure 6(a) the viscosity-velocity results fall into two general groups of solvents which occur on parallel but separate lines. These groups are

- Aqueous and alcoholic solutions
- Dimethyl sulfoxide, acetone etc.

We shall consider here the possibility that these groupings result from differences in the chemical behavior of unpassivated titanium in these solvents. The most important factors would appear to be the stability of hydrogen, the stability of titanium ions in the solvent and the presence and type of bonding of oxygen in the solvent.

Hydrogen chemistry is different in the various solvents. Aqueous and alcoholic solutions are somewhat similar in that they both have a great deal of hydrogen bonding, the hydrogen is present in -OH groups (except for the methyl hydrogens), and hydrogen gas may be liberated upon cathodic polarization of an electrode. In dimethyl sulfoxide, acetone and several of the solvents in the second group, hydrogen is present in inert methyl ($-CH_3$) groups, there is little hydrogen bonding, and solvent reduction may occur without hydrogen generation. Even when hydrogen gas is generated, it occurs at very negative potentials (more negative than -2 volts) of an aqueous saturated calomel electrode. In our tests the open circuit potential of a specimen containing a propagating stress corrosion in these latter solvents was observed to be only -200 mV ($\pm$200 mV) versus an aqueous saturated calomel electrode. It

should be noted that velocities of cracking in neutral chloride aqueous solutions, in the "anodic protection" region (at room temperature) is the same magnitude as for the second group of solvents. In the "anodic protection" region, hydrogen is not generated (on the outer specimen surface at least). The major exception to this grouping of solvents is the formic acid solution. It falls into the dimethyl sulfoxide group of solvents on the basis of the velocity-viscosity correlation, but hydrogen gas is generated at low cathodic polarization voltages on active metal surfaces. On a high-overvoltage metal (such as one which is passivated), reduction of formic acid takes place without hydrogen generation.

The ionic solution characteristics in the various solvents are different i.e., energies, number of solvation molecules, etc. This kind of chemical influence would lead to differences in transport properties (conductivity, diffusion coefficients) and in thermodynamic properties. Sedricks and Green (31) have used these differences in an attempt to exclude the chloride ion as a stress corrosion agent by comparing behavior in 0.6 M LiCl aqueous and DMSO solutions. The much faster crack velocities observed in the water solution are attributed to the ease of hydrogen reduction and it was concluded that the low velocities in DMSO solutions indicated that the chloride ion played a minor role in the cracking process. Several factors probably make this analysis an oversimplification; for example, although the chloride ion is solvated to a lesser degree in DMSO and thus could be considered "freer" the mobility of the ion on an absolute scale is lower than in water (see conductivity results). Also, the concept of unsolvated anions (i.e., Cl^-) in DMSO proposed by Parker (32) was developed from low solution concentrations.

Little is known about the relative oxidation rates which might be observed in these solvents. However, the thermodynamic properties of dimethyl sulfoxide for example (33), lead one to predict that potentially it is a better oxidizing agent than water (34), as are also acetone and formic acid (34). This could lead to faster passivation of a fresh Ti surface in these solvents. It would certainly indicate that Ti^{+3} species would be less stable (with respect to oxidation) in these solvents than in water. More will be said about this below.

The possibility that the two general groupings of solvents in the velocity: viscosity correlation might be the result of different titanium chemistry was suggested by the known relative stability of Ti^{+3} solutions in water and in dimethyl sulfoxide. In aqueous solutions of pH 1 or lower, Ti^{+3} (aqueous) is stable indefinitely if protected from atmospheric oxygen. On the other hand, acidified $TiCl_3$ reacts vigorously with DMSO to give a yellow solution with a very foul odor (see also (35)). The reaction is most likely the oxidation of Ti^{+3} to an oxychloride species of valence 4, accompanied by the reduction of DMSO to dimethyl sulfide. We have tested the other solvents and found that only methanol and glycerine did not react with acidified $TiCl_3$ al all, although some reacted rather slowly. Of course, lower valent titanium species would not be stable in any of the solvents ([36])(in which the aqueous chemistry of titanium is discussed). Another observation which may have some importance, is that "anodic protection" in aqueous HCl solutions occurs in the potential range where $(TiO^{2+})_x$ (or an oxychloride) is stable, rather than Ti^{+3}. Also, the velocity at such potentials is in the scatterband for the DMSO group of solvents. The importance of these results could be that anodic processes involving the formation of Ti^{+3} or $(TiO^{2+})_x$ are important to the crack extension, and in conditions where $(TiO^{2+})_x$ is formed, the cracking is slower than for those conditions where Ti^{+3} is formed.

Thus, we may conclude:

- Differences in the ease and rate of hydrogen production could lead to the observed behavior in the various solvents, i.e., if one postulated as hydrogen embrittlement process. However, the formic acid results are not consistent with this generalization.
- Differences in oxidation rates of a fresh titanium surface in the various solvents could contribute to the two groupings, but there is insufficient information about the kinetics of oxidation to provide a quantitative evaluation.
- Differences in solvation do not seem to be an appropriate explanation for the variation in behavior, although not enough

is known about physical properties of the concentrated solutions used here to come to any firm conclusion.

- Differences in stability of Ti^{+3} versus $(TiO^{2+})_x$ are consistent with the different cracking rates observed in the two groups.

Influence of Potential

In this section we shall discuss the influence of the electrical potential on crack growth (in Region II) in the "anodic protection" and "cathodic protection" regions in aqueous solutions. Neutral chloride solutions show both regions of behavior, with the maximum crack growth rates at about -200 mV (versus SCE), which then decrease with a change of potential in either direction (see Fig. 7). A more complete discussion of the influence of metallurgical, potential and temperature effects is presented in reference 17.

In the range of potentials more negative than -200 mV (versus SCE), the velocity was observed to decrease until there was no propagation ($v_{II} \sim 10^{-6}$ cm/sec) at -1500 mV and more negative. This behavior has been previously reported for bromide and iodide solutions as well, but at a different concentration (1). In Figure 10 it may be noted that cathodic protection is also observed in very basic solutions, but not in very acidic solutions. At the same time, it was observed that hydrogen evolution on the bulk surface of the specimen was quite vigorous in 9 M HCl at -400 to -600 mV (versus SCE) and more negative, while we had to go to about -1200 mV to achieve the same level of hydrogen evolution in neutral solutions, and to even more negative potentials for the basic solution. This is consistent with the expected shift in equilibrium potential of the $H^+ \rightarrow H_2$ reaction with pH.

We propose that the absence of cathodic protection in concentrated HCl (and HBr and HI) is associated with the hydrogen evolution, and may be explained by a current distribution argument, as follows. For a reaction under ohmic control, as the hydrogen ion reduction is at -500 mV in concentrated HCl, the current distribution will be such that most of the current will flow to the external surface of the specimen, and very little will flow into the

crack. Within the crack, the current will be highest at the outermost parts of the crack. As the current is small on the walls in the tip region of the crack, the tip will not be as highly polarized as the outer part of the specimen (the difference being due to an iR drop in solution). In fact, the potential near the tip cannot be changed by changing the external potential in such a situation, and one has a constant electrochemical condition (potential) at the crack tip. This would lead to a constant crack propagation velocity which would not change with a change of external potential. The potential near the tip is then a mixed potential, or (more probably) the potential at which the ohmically-controlled reaction goes into the region of nonohmic (i.e., kinetic) control. The velocity in HCl should level out at about the potential where the reaction (H_2 evolution) becomes ohmically controlled, and this is exactly what is observed. On the other hand, the velocity in neutral and basic should still be sensitive to the external potential until the condition is reached where H_2 evolution is again ohmically controlled, at which point the velocity should level out again. Our observations are consistent with the first part of this statement, but we have not tried to verify the latter part. This current distribution argument does not provide an explanation for cathodic protection as such, but does suggest why it is not observed in acidic solutions. On the other hand, anodic (dissolution) mechanisms would be consistent with these cathodic protection results. The results on the highly basic solutions also indicate that the postulate that high concentrations of OH^- ions at the crack tip produce cathodic protection is incorrect. We consider that it is unlikely that a pH gradient from a pH of 0-1 (at the crack tip) to 14.5 in the bulk solution exists although this has not been checked experimentally.

"Anodic protection" is observed in chloride solutions independent of pH. Bromide solutions exhibit it also, but to a lesser extent, and iodide solutions do not exhibit anodic protection at room temperature.

There is the additional experimental observation that anodic protection is not observed (even in chloride solutions) for alloys and heat treatments which exhibit SCC velocities faster than 2×10^{-2} cm/sec. at a potential of -200 mV.

The absence of anodic protection in iodide solutions may be due to the ohmically controlled oxidation of iodide to iodine, in which case a current distribution argument would again be appropriate. It is experimentally observed that the oxidation of iodide is ohmically controlled (on the external surface) at potentials more positive than +100 mV (versus SCE) in ∿5 M solutions-consistent with a current distribution argument. (This does not explain why the velocity increases between potentials of -200 and +100 mV.)

The anodic protection region in 9 M HCl (aqueous) begins at one end at about the potential where hydrogen ion reduction is known to stop. One could immediately jump to the conclusion that this indicates that hydrogen is responsible for the cracking process at more cathodic potentials. However, this hardly appears tenable when the neutral and basic chloride solutions are also considered. In the basic solutions in particular, the equilibrium potential for the hydrogen ion-hydrogen gas couple is about -1100 mV (versus SCE) at pH 14.5. However, anodic protection at this pH was found to occur at about the same potential as for acidic and neutral solutions (see Fig. 10). One might expect some difference in concentration between bulk solution and the solution within the crack, but it could hardly be large enough to allow the same crack tip pH for bulk solution pH's from 0 to 14.5. We conclude therefore, that it is unnecessary to consider the hydrogen reaction in explaining anodic protection.

The reaction

$$Ti^{+3} + H_2O \rightleftarrows (TiO^{2+})_x + 2H^+ + e^-$$

occurs at potentials more positive than about 0 mV (versus SCE) at a pH of 0, which is the potential for the onset of anodic protection. Other evidence that the formation of the four-valent species might have been responsible for the retardation is as follows:

(1) A yellow-green solution was observed to stream from the crack into the bulk solution at these potentials. This is probably a solution of the oxychloride of four valent titanium.

(2) On the velocity-viscosity plot, Fig. 5(a), solutions in

in which four valent Ti is stable lie below those in which Ti^{+3} is stable, and this includes the anodic protection results.

Evidence against the relative stability of Ti^{+3} - TiO^{2+} as being responsible for the occurrence of anodic protection, is listed below.

(1) Anodic protection is virtually independent of pH, but the titanous-titanyl reaction is strongly dependent on pH. That is, $(TiO^{2+})_x$ is not stable in neutral solution, with respect to precipitation of TiO_2, and apparently there is no three-valent Ti species formed at any potential at pH 14.

(2) There is no evidence of anodic protection in methanol solutions of LiCl (1) where both +3 and +4 species should be stable. However, there is the complication of pitting in these solutions at low anodic potentials.

Thus, we are left with no really satisfactory explanation of anodic protection apart from a few rather vaguely formulated ideas. It was noted above that in specimens that do not exhibit anodic crack retardation,the velocity of cracking at -200 mV is greater than 2×10^{-2} cm/sec. The results reported here for 9 M LiCl solutions at 112°C fulfill this requirement. Also, as mentioned previously, the present Ti-8-1-1 when heat treated to precipitate α_2 particles in the α phase, shows cracking in 9 M LiCl at room temperature above 2×10^{-2} cm/sec. and no anodic protection. This suggests that a relative kinetic effect is being observed, i.e., competition between two (or more) processes such as oxidation versus stress corrosion cracking. In situations where oxidation of the surface is fast enough, it may stifle the cracking process. If cracking is fast enough, it may create its own conditions which are not significantly changed by any oxidation. This rather vague formulation has some addition support from the observation that at these anodic potentials, the retarded crack tends to "tunnel." Further, an analogous phenomenon is also observed in corrosion fatigue in a similar alloy, where the effect of potential is to cause the $\frac{da}{dt}$ versus ΔK curves to cross one another (37). This suggests that attainment of the bulk surface properties destroys the conditions for stress corrosion cracking.

Summary

Experimentally it was established for the conditions investigated, i.e., Ti-8Al-1Mo-1V (820°C WQ) tested in solvents containing chloride, bromide or iodide ions, that

(i) The Region II plateau velocity varies inversely with the viscosity

(ii) The activation energy for the Region II plateau velocity shows the same temperature dependence and numerical values as that for velocity

(iii) The plateau velocity in the several solvents may be correlated with the solution conductivity

(iv) Mixing the solvents gives nonadditive results both on viscosity and conductivity basis

Theoretical consideration of these results have shown that no simple explanation of the limiting propagation velocity can be proposed based on

- Hydrogen diffusion in the metal
- Limitation of the velocity by fluid flow cavitation during crack extension
- Limitation by a chemical reaction under ohmic control
- Limitation by a process involving a mass transfer controlled chemical reaction.

It is possible that a combination of these processes may be capable of providing an explanation. Some indication of chemical effects which have to be considered have been presented.

It is proposed that

- The absence of cathodic protection in acidic aquaous solutions is due to ohmic control of the hydrogen discharge reaction which "isolates" the crack tip from external potential control.
- Anodic protection may be due to a relative kinetic effect.

REFERENCES

1. Blackburn, M. J., Feeney, J. A., Beck, T. R., "Stress Corrosion Cracking of Titanium Alloys", *Advances in Corrosion Science and Engineering*, R. W. Staehle, Ed., Plenum Press (in press).

2. Blackburn, M. J., Smyrl, W. H., Feeney, J. A., "Engineering Aspects of Stress Corrosion Cracking of Titanium Alloys", *Status of SCC of High Strength Alloys*, Ed. B. F. Brown, Government Printing Office (in press).

3. Fager, D. N., Spurr, W. F., *Corrosion*, 26, 1970, p. 409.

4. Sedricks, A. J., *Corrosion*, 25, 1969, 207.

5. Beck, T. R., Blackburn, M. J., Speidel, M. O., "Stress Corrosion Cracking of Titanium Alloys: SCC of Aluminum Alloys, Polarization of Titanium Alloys in HCl and Correlation of Titanium and Aluminum SCC Behavior", Contract NAS7-489, Quarterly Progress Report 11, March 1969.

6. Sandoz, G., Newbegin, H., Report of NRL Progress, May 1968, p. 31.

7. Meyn, D. A., Report of NRL Progress, March 1971, p. 16.

8. Smyrl, W. H., Blackburn, M. J., in Proceedings of Conference on Stress Corrosion Cracking Mechanisms in Titanium Alloys, Atlanta, 1971, to be published.

9. Mostovoy, S., Ripling, E. J., Crosley, P. B., *Journal of Materials* 2, 1967.

10. Robinson, R. A. and Stokes, R. H., *Electrolyte Solutions*, 2nd Ed., (revised) Butterworths, London, 1965.

11. Schlafer, H. L., Schaffernicht, W., *Angew. Chem.* 72, 618 (1960).

12. Moynihan, C. T., Balitactac, N., Boone, L., Litovitz, T. A., *J. Chem. Phys.* 55, 3013 (1971).

13. Chapman, T. W., Newman, J., "A Compilation of Selected Thermodynamic and Transport Properties of Binary Electrolytes in Aqueous Solution", UCRL-17767, Univ. of California, Berkeley, 1967.

14. Beck, T. R., "Stress Corrosion Cracking of Titanium Alloys, Preliminary Report on Ti-8Al-1Mo-1V Alloy and Proposed Electrochemical Mechanism", Boeing Doc. D1-82-0554, 1965.

15. Brown, B. F., Fujii, C. T., Dalberg, E. P., *J. Electrochem. Soc.*, 116 1969, p. 218.

16. Powell, D. T., Scully, J. C., *Corrosion*, 24, 1968, p. 151.

17. Blackburn, M. J., Smyrl, W. H., "Stress Corrosion Cracking of Titanium Alloys - A Review of Recent Developments", presented at the 2nd Intn. Conference on Titanium, Boston 1972, to be published in proceedings.

18. Beck, T. R., in "The Science, Technology and Application of Titanium", Ed. R. Jaffee and N. Promsel, Pergamon Press, 1970.

19. Scully, J. C., to be published in proceedings of the Intn. Conference on Stress Corrosion Mechanisms in Titanium Alloys, Atlanta 1971.

20. Beck, T. R., in "The Theory of Stress Corrosion Cracking of Alloys", Ed. J. C. Scully, NATO, Scientific Affairs Div. Brussels 1971.

21. Beck, T. R., Blackburn, M. J., Smyrl, W. H., NAS7-489, Quarterly Report No. 20, June 1971.

22. Pourbaix, M., "Atlas of Electrochemical Equilibria", Pergamon Press New York, 1966.

23. Rostocker, W., McCaughey, J. M., Markus, H., "Embrittlement by Liquid Metals", Reinhold, New York, N. Y. 1960.

24. Newman, J., Smyrl, W. H., "Fluid Flow in a Propagating Crack," to be published.

25. Taylor, G. I., *Journal of Fluid Mechanics*, 18, 1963, p. 595-619.

26. Temperley, H. N. V., *Proc. Physical Soc.*, 59, 147, 199.

27. Tennyson Smith, *Corrosion Science*, 12, 1972, p. 45.

28. Newman, J., Hseuh, L., "Currents Limited by Gas Solubility", UCRL-19098, Univ. of Calif., Berkeley, 1970.

29. Clark, R. J. H., "The Chemistry of Titanium and Vanadium", Elsevier Press, New York, N. Y., 1968.

30. Beck, T. R., Grens, E. A., *Journal Electrochem. Soc.*, 116, 1969, p. 177.

31. Sedricks, J. A., Green, J. A. S., "Critical Species in the Transgranular Stress Corrosion Cracking of Titanium Alloys in Aqueous Solutions", RIAS Report to be published in Corrosion.

32. Parker, A. J., Quarterly Reviews, 1962, p. 163.

33. Mackle, H., O'Hare, R. A. G., *Trans. Faraday Soc.*, 58, 1962, p. 1912.

34. Latimer, W. M., "Oxidation Potentials", 2nd Edition Prentice Hall, N. J., 1952.

35. Melendres, Ca. A., M.S. Thesis,Univ. of Calif., Berkeley 1965 (UCPL-16330).

36. Cotton, F. A., Wilkenson, G., "Advanced Inorganic Chemistry, A Comprehensive Text", Interscience, New York, 1967.

37. Speidel, M. O., Blackburn, M. J., Beck, T. R., Feeney, J. A., to be published in *Proceedings of the Inernational Conference on Corrosion Fatigue*, Storrs, Conn., 1971.

4.2 PITTING OF TITANIUM ONE-DIMENSIONAL PIT EXPERIMENTS

In prior studies on pitting of titanium (1) it was observed that pits grown on foil were initially approximately hemispherical as observed for other metals (2,3,4). After the pits penetrated the foil, corrosion continued at the periphery of the holes with no apparent change in mechanism. The new corroding areas were nearly cylindrical and at right angles to the foil faces. A further simplification from a cylindrical to a planar surface would allow a one-dimensional analysis of the mass-transport phenomena.

Planar corrosion was obtained on the ends of small diameter rods or rectangular prisms of titanium which were cast in epoxy resin like the lead in a pencil. This technique of insulated cylinder has been reported previously (5) with larger diameter specimens of copper in studies of electropolishing.

4.2.1 Experimental

General - Commercially-pure, A-75, titanium from Titanium Metals Corp. was used for the experiments. Cross sections of three different size specimens were 0.163 cm diameter, 0.1 x 0.1 cm and 0.16 x 0.32 cm and the lengths were 3 to 6 cm. The specimens were cast in epoxy resin with an outside diameter of 0.6 cm. The working end of each titanium "pencil" was ground flat with silicon carbide paper on a belt sander before each experiment.

All experiments were conducted with the titanium in the anode-facing-up position. Most of the experiments were done in an inverted cut-off polyethylene bottle with the titanium "pencil" mounted in a rubber stopper similar to the arrangement in (5). Electrolyte filled the cell to a level about 1 cm above the end of the "pencil". Events in the "pit" formed at the working end of "pencil" were observed through a B&L binocular zoom microscope at 7 to 35 X. The cell was potentiostated using a Wenking Model 66TS1 and platinum counter electrode and saturated calomel electrode (SCE) reference. All potentials cited in this paper are in respect to the SCE. Most of the potential drop in the cell was within the "pit", so the location of the counter and reference electrodes was not important electrically and they could be located at the side of the cell out of the way of the microscope.

All experiments were conducted at room temperature (21°C) unless otherwise specified. All chemicals used were Bakers reagent grade without further purification. Solutions were made with commercially supplied distilled water.

Cell current and electrode potential were displayed on a Hewlet-Packard strip-chart recorder and X-Y plotter.

Potential vs. Pit Depth - As is appeared important to determine the magnitude of the potential drop in the pit electrolyte, a cell illustrated in Fig. 1 was designed for this measurement. The cell was made of Plexiglas pieces cemented together. The titanium pencil was fitted in the bottom of the cell with threaded Teflon sleeve. An annular platinum disk counter electrode was axial to the titanium pencil. The titanium pencil was potentiostated in respect to a calomel reference electrode mounted in the cell.

A scale drawing of the Luggin capillary in the artificial pit showing the important dimensions is given in Fig. 2 . The cross sectional area of the tip was 2.4% of the area of the pit. Measurements of potential vs. position were made over a range of pit depths from 0.07 to 0.12 cm. At a distance above the pit the capillary flared out to a shaft diameter of 0.1 cm that fitted into a Plexiglas bushing mounted on split titanium leaf springs. A sliding fit sealed with stopcock grease was used in order to avoid breaking the capillary tip when it hit the electrode at the bottom of the pit.

The Plexiglas bushing mounted on split leaf springs of titanium maintained axial alignment of the Luggin capillary. The bushing and capillary were forced down against the spring by a micrometer head mounted on top of the cell. A Teflon tube filled with electrolyte connected the Luggin capillary-bushing assembly to a calomel electrode in a reservoir outside of the cell. The signal from this calomel electrode was fed into Keithly model 610B electrometer.

A Helipot connected as a voltage divider across a mercury cell provided an electrical analog signal of the Luggin capillary position. The helipot

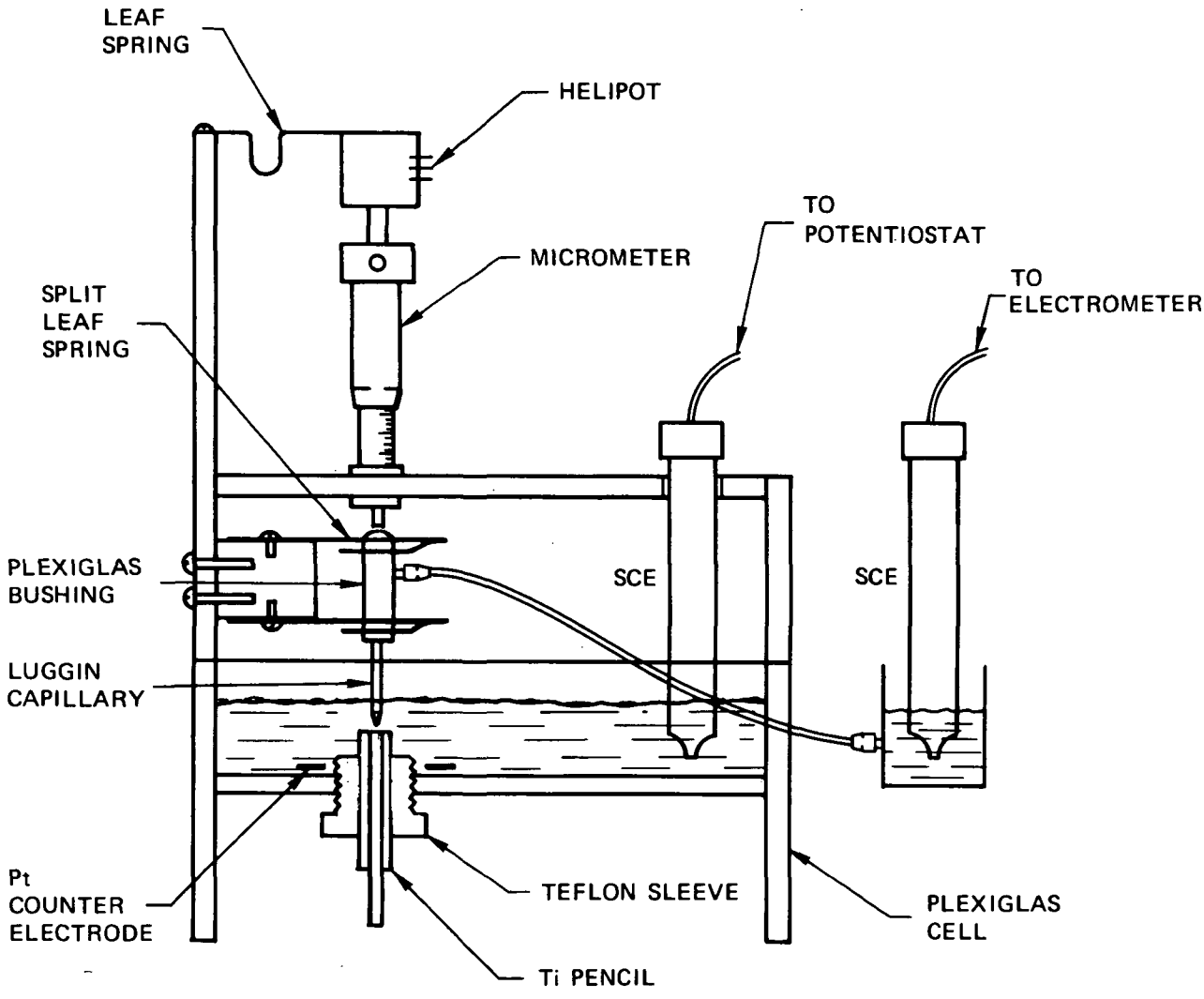

Fig. 1 - Cell for Measuring Potential Drop in Pit Electrolyte.

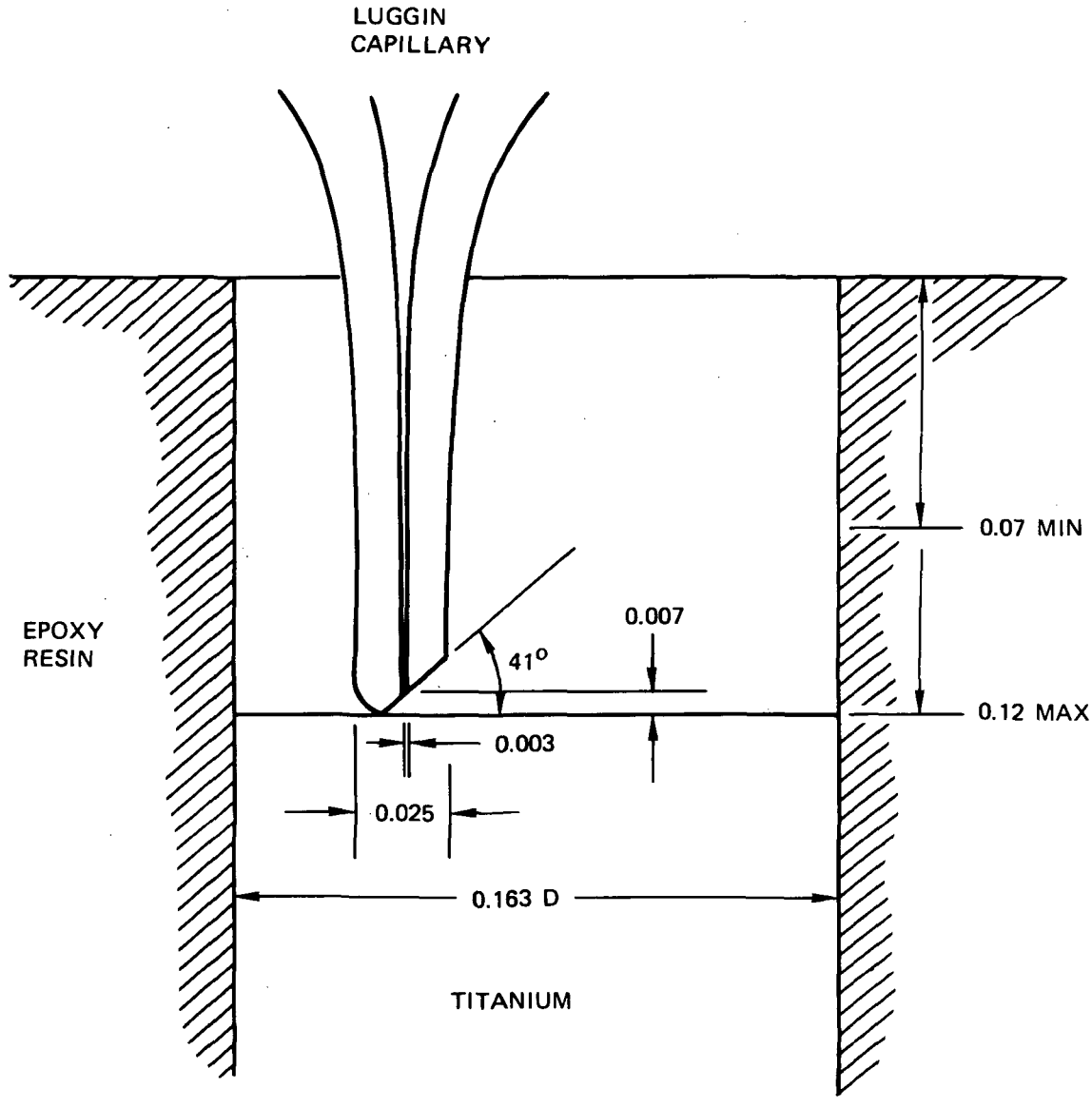

Fig. 2 - Scale Drawing of Luggin Capillary in Artificial Pit - Dimensions in cm.

was attached to the cell through a leaf spring which allowed axial movement but prevented rotation and the shaft was connected to the micrometer. The signals from the Helipot and from the electrometer connected to the SCE from the Luggin capillary were displayed on the X-Y plotter. The Helipot signal, which was linear with Luggin capillary position, was calibrated with the micrometer. During the experiments periodic checks of Luggin capillary position and pit depth (seen through the epoxy resin) were made with a cathotometer.

Open-Circuit Potential Transients - The pattern of decay of potential of a working electrode with time after open circuiting is diagnostic in determining the type of potential drop, e.g., electrolyte ohmic drops should disappear immediately while activation overvoltage should decay with log time (6).

A titanium pencil was potentiostated in a polyethylene cell. The circuit was opened by a Stevens Arnold, Inc. millisecond relay on the counter-electrode side. The signal from a separate calomel electrode in the cell was fed into a Tektronix model 510 oscilloscope for short-time transients and through the electrometer to the stripchart to record longer period transients.

For each applied potential to the specimen a series of open-circuit transients was photographed on the oscilloscope screen at sweep speeds a decade apart from 10 μsec/cm to 100 msec/cm. The stripchart was used to obtain data out to 10 sec. or more. This procedure gave some overlap for each scale when the data were replotted on a semilog graph.

Identification of Gas from Pits - A small amount of gas was observed to emanate continually from the pits. An experiment was devised to determine if the gas was hydrogen or oxygen. It was collected in a section of 1 ml burette with a flared end filled with water and inverted over an artificial pit. After a few tenths of a ml of gas were collected, either hydrogen or oxygen were introduced. The gas mixture was sparked with platinum electrodes at the top of the burette and change in volume was determined.

Photographs - Photographs of the corroded surfaces were taken with an Ultrascan model SM-2 scanning electron microscope (SEM).

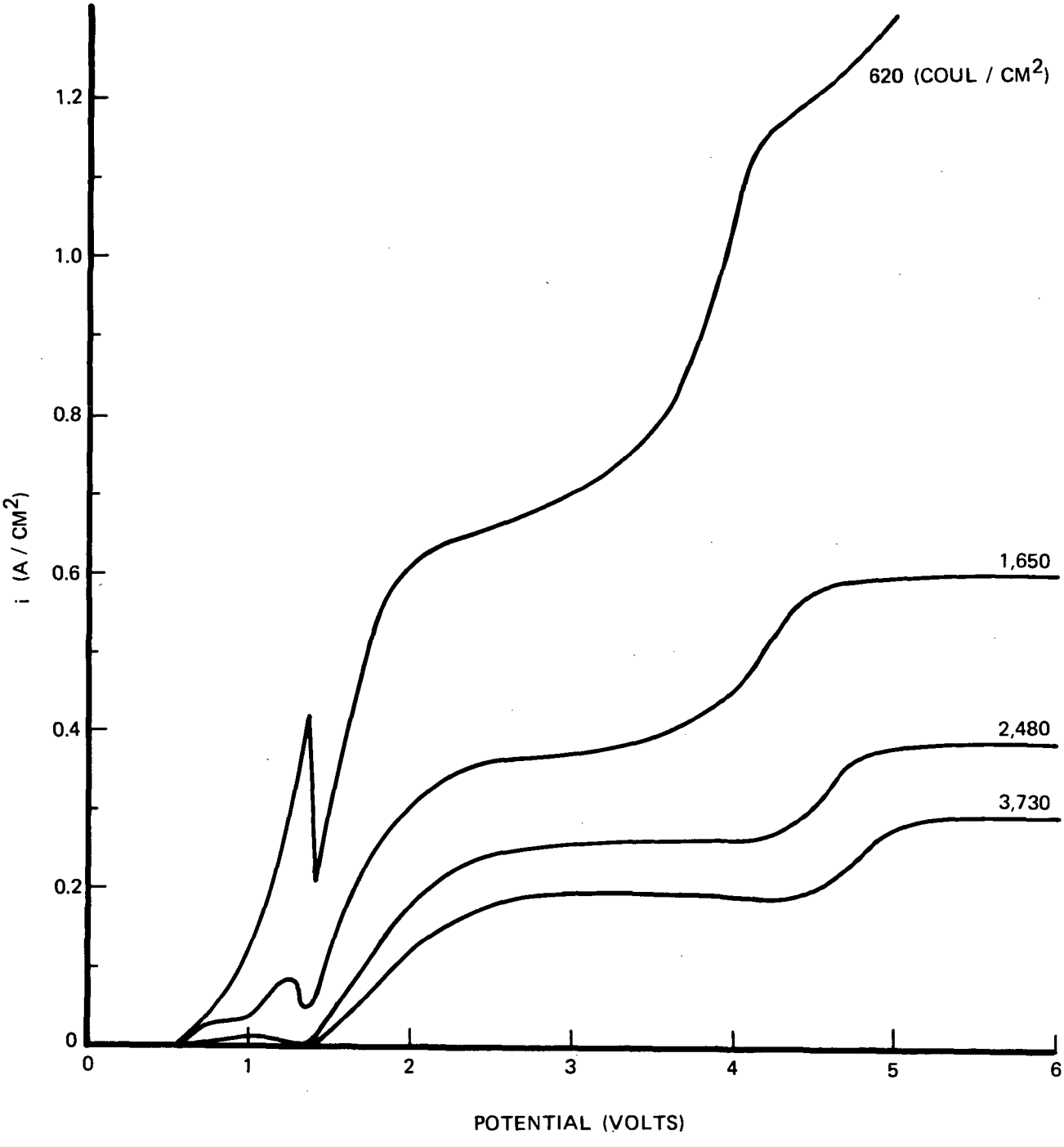

Fig. 3 - Current Density - Potential Curves for 10^{-2} Titanium Electrode in 1 M KBr - Parameter is Amount of Charge passed.

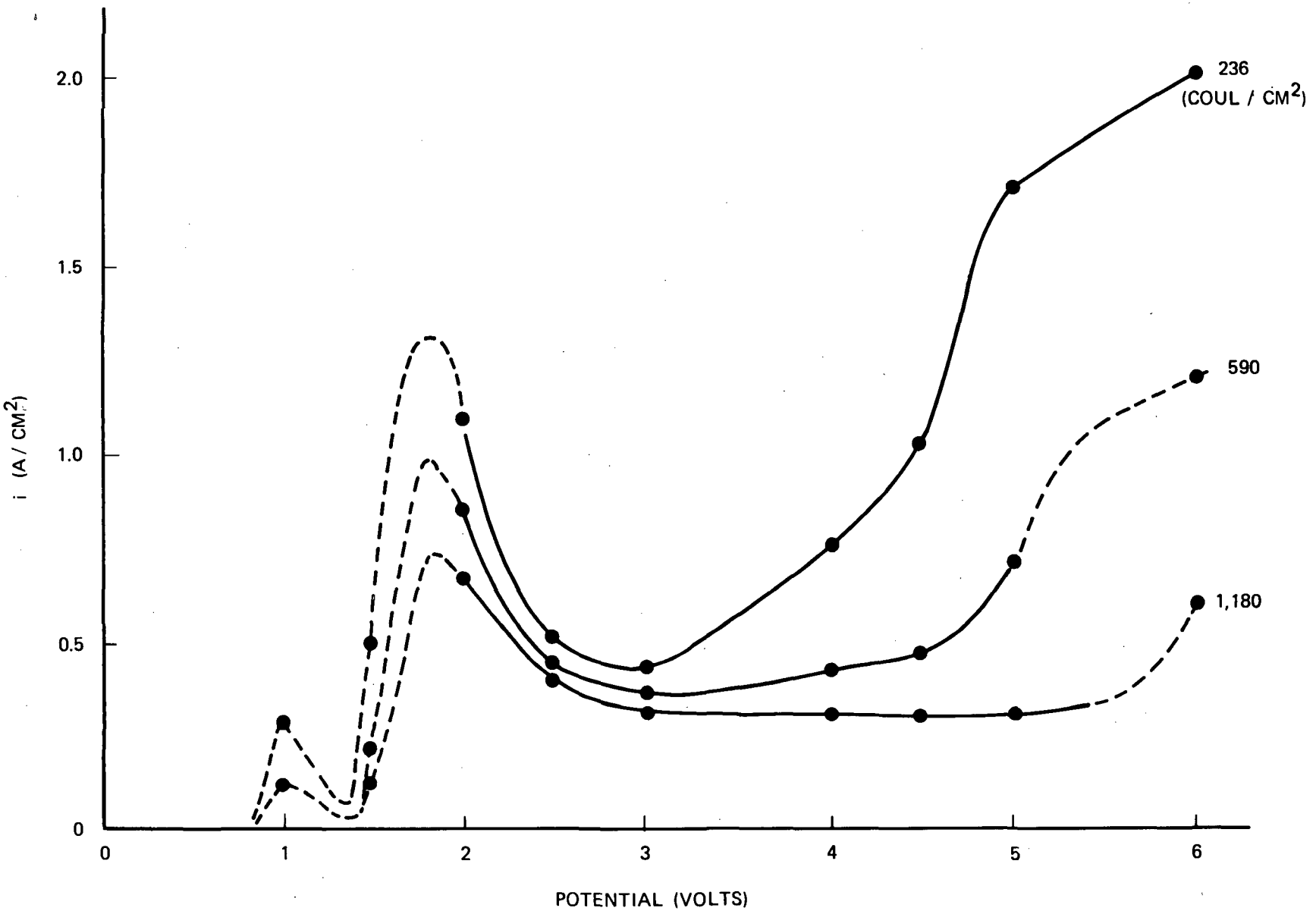

Fig. 4 - Current Density - Potential Curves for 0.05 cm^2 Titanium Electrode in 4.4 M HBr - Parameter is Amount of Charge passed.

4.2.2 Results

Current - Potential Curves - A typical series of current-potential curves is shown in Fig. 3 for pitting of the 0.1 x 0.1 cm titanium pencil in 1 M KBr. These curves, obtained with a sweep rate of about -20 V/min, were taken at various times during propagation of a pit at a potential of 6.0 V. Amount of charge passed up to the time of the measurement is the parameter.

Three regions are observed: a hump between the pitting potential and 1.4 V, a plateau between about 2.0 V and 3.5 to 4.5 V and a second plateau about 4.0 to 5.0V-- at least out to 17 V. These will be referred to as the hump, the lower plateau and the upper plateau, respectively. At slower sweep speeds the maximum of the hump occurs at a potential approaching 0.98 V and the steady-state pitting potential is 0.9 V. With elapsed time or charge passed the current density in all three regions decreases and the half-wave potential between the lower and upper plateaus increases. The minimum between the hump and the lower plateau tends to remain constant at 1.4 V. A positive sweep rate gives similar shaped curves except that a second hump in current density occurs on the lower plateau at 1.8 V.

Current-potential curves for more nearly steady-state conditions for a 0.16 x 0.32 cm titanium pencil in 4.4 M HBr are shown in Fig. 4. These curves were constructed from constant-potential experiments with interpolations for three charge densities. The current density decreased in these runs over a range of 0 to -1.7 power of the charge density depending on potential and charge density. The large negative slope was related to the change from the upper to the lower plateau.

Above room temperature (50° and 77°C) strong oscillations occurred between 0.9 and 1.5 V in 4.4 M HBr solution. The frequency was about 10 cycles per minute.

The character of the corroding surface was different in the three regions. At the hump and up to a potential somewhere between 1.5 and 2.0 volts the pit was covered with what looked like a layer of compact gray mud. The metal surface after cleaning ultrasonically or by cathodic hydrogen evolution

was very porous as can be seen in the SEM photograph at 1000 X in Fig. 5 (enlarged for reproduction).

On the lower plateau an orange-to-white precipitate was formed and extruded from the pit. The outer surface was chunky and white and the chunks slowly dissolved in the HBr solution. Deeper in the pit the material was orange and appeared to be somewhat gelatinous. Most of the material was easily removed with a jet of water after the experiments except for a thin film that adhered to the surface. After washing this film with acetone and drying it usually cracked and peeled off. The underlying metal surface appeared bright and crystallographically etched under the 35 X binocular microscope. A SEM photograph at 1000 X in Fig. 6 shows the faceting and what look like terraces.

On the upper plateau a viscous orange solution covered the bottom of the pit and a shiny surface could be seen through it. With time the solution became translucent and the metal surface could no longer be seen. In washing out the pit material as above a salt film adhering to the metal was also observed. The underlying metal was polished as can be seen in the SEM photograph at 100° X in Fig. 7. In spite of being polished, it can be seen that there remained some differential metal removal between different grain faces. Some round bumps also covered the surface.

Good leveling of the titanium surface, as opposed to the above micro texture, occurred in bromide solution at all potentials as the pits deepened. Initially, when a potential above 2.5 V is applied to a sanded pencil end the corrosion starts uniformly at the periphery of the titanium. The gelatinous corrosion product spreads inwardly until the whole surface is active. Corrosion is initially greater at the periphery of the titanium as would be expected from consideration of ohmic current density distribution. As the pit deepens the surface becomes very level and at right angles to the epoxy resin walls. The surfaces were not usually so level in chloride and iodide solutions.

Stirring the precipitate in the pits with a glass micro stirring rod always caused the current to increase in all three regions. Sometimes the small gas bubbles (0.001-0.01 cm diameter) agglomerated into a larger bubble

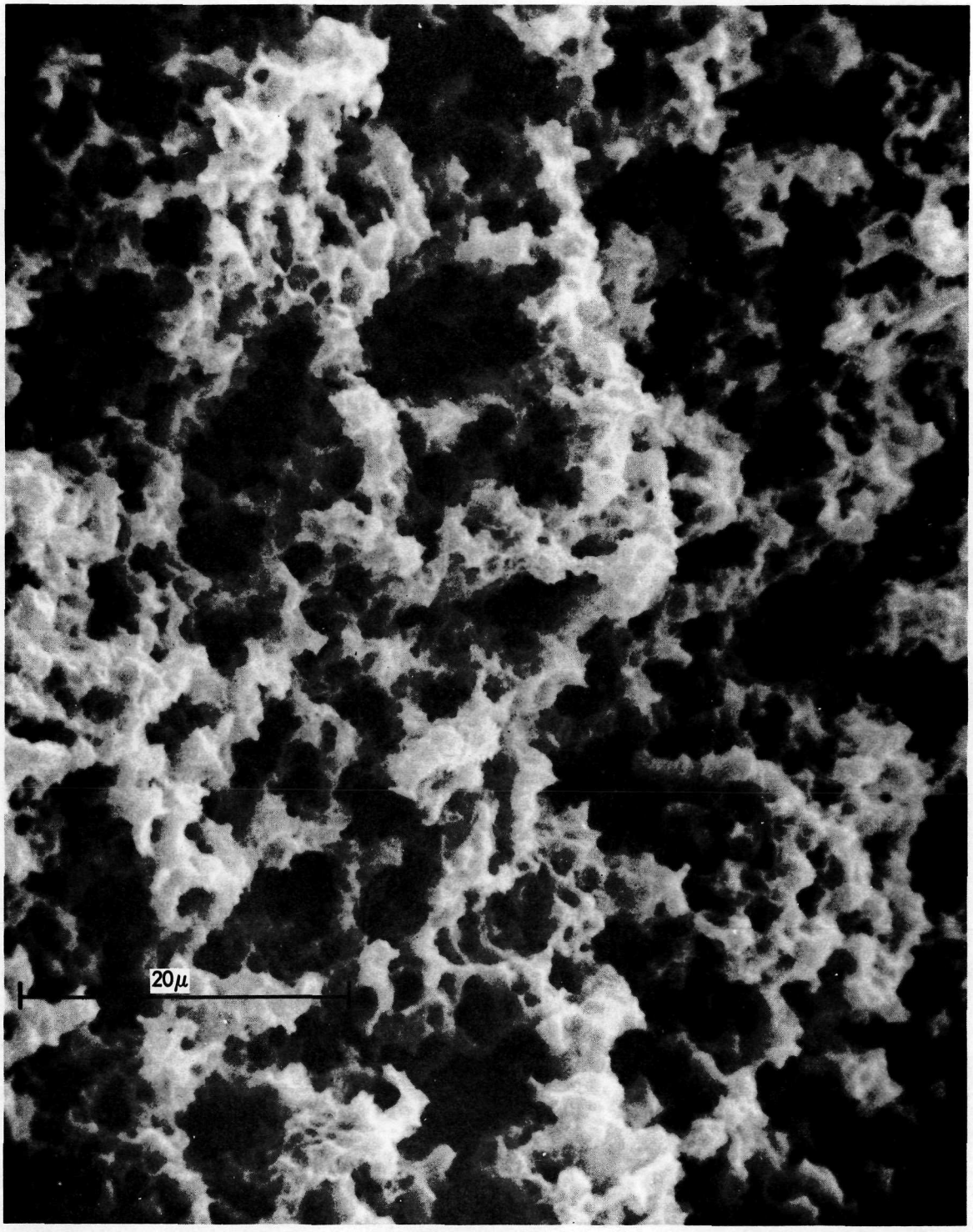

Fig. 5 - SEM Photograph of Titanium Surface pitted at a Potential of 1.5 V.

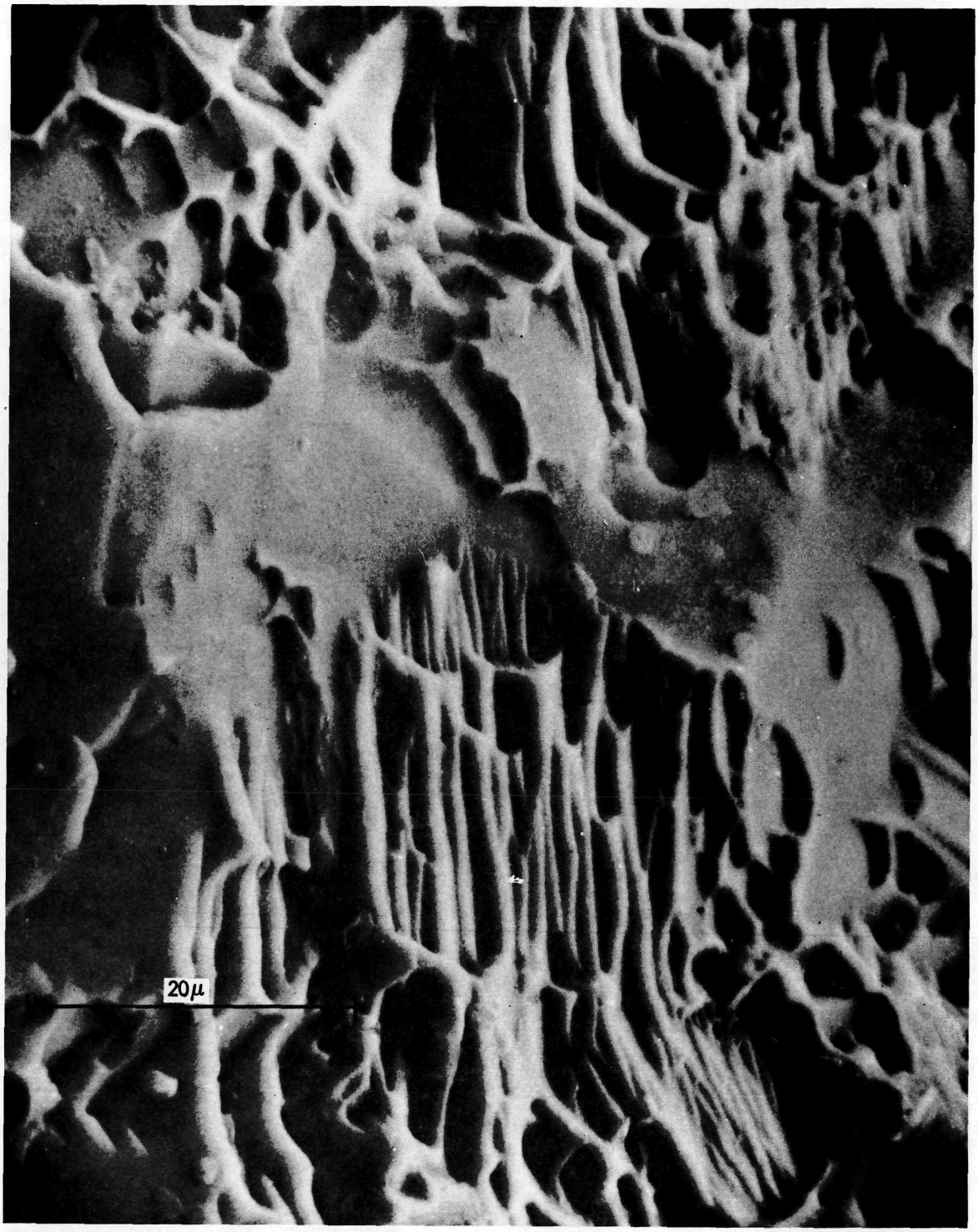

Fig. 6 - SEM Photograph of Titanium Surface pitted at a Potential of 3.0 V.

Fig. 7 - SEM Photograph of Titanium Surface pitted at a Potential 6.0 V.

that filled the pit and forced out the precipitate. Current decreased during the growth of these bubbles and increased on their release. In switching from the upper plateau to 1.5 V such a conglomerate bubble always formed. As it pushed up the precipitate a layered structure could be observed. Typically there was a compact layer about 10^{-3} cm thick with a columnar layer about 10^{-2} cm thick above.

Generation of Gas - Volumetric measurements with the gas burette during pitting of titanium pencils in chloride solutions are given in Table 1. Chloride solutions were used because the higher current density therein gave an adequate gas generation rate, whereas the gas generation rate was very low in bromide solutions. Only three possible gases, hydrogen, oxygen or chlorine, could be generated in the pit under these conditions and the experiments were designed to determine which one it was.

Column 1 of Table 1 gives data for the gas collected from pitting in 1 M HCl. The gas was sparked after collection, giving a decrease in volume indicating a combination of part of the gases. Hydrogen was then added from a platinum wire cathode in the same solution. No change in volume occurred on sparking, indicating that there was no residual oxygen (or chlorine) in the gas after the first sparking. The gas burette was then transferred without spilling to a cell with 1 N H_2SO_4 electrolyte and oxygen was collected from a platinum wire anode. After sparking, the volume decreased. After adding further oxygen and sparking again, the volume further decreased as noted in column 1a. These results show that the gas from the pit was predominantly hydrogen but some oxygen (or chlorine) was also present.

Column 2 gives data for gas collected from an alkaline chloride solution in order to eliminate the possibility of chlorine being present. The solution was boiled in a flask to remove dissolved air and then cooled and poured into the cell with a minimum of agitation to minimize further air dissolution. A decrease in volume of the collected gas occurred on sparking showing that again a mixture of combustible gases was present. The burette was then transferred without spilling to a preboiled and cooled 0.3 M Na OH solution in which oxygen was collected from a platinum wire anode.

The gas was sparked during collection of oxygen and the volume decreased linearly with time then increased linearly at the same rate. An amperometric equivalence point was thereby obtained at a residual volume of 0.095 cm^3. The residual gas is assumed to be nitrogen from air that redissolved in the solutions.

Column 3 shows the results of an experiment in which hydrogen was collected from a platinum wire cathode in preboiled 0.3 M NaOH solution. Sparking again caused a slight decrease in volume. Addition of oxygen from a platinum wire electrode in the same solution with simultaneous sparking gave a linear decrese in volume followed by a linear increase with an equivalence point at a residual volume as above. In this case there can be no doubt that the residual gas was nitrogen from dissolved air. A calculation of mass transfer rates of gases from bubbles to solutions (7) confirms that the experimental observations are reasonable. A more sophisticated gas analysis method might have been used but it would have been subject to the same problems of mass transfer.

It appears that hydrogen is the dominant gas, if not the only gas issuing from these pits. A rough estimate of the amount from the above experiments and by making counts of bubbles gave an estimated coulombic equivalent between 0.01 and 0.07 that of the anodic current in chloride and in bromide solutions. In general there appeared to be a greater gas evolution rate at lower potentials and higher temperature.

Potential Traverse in Pit - A typical potential traverse for the Luggin capillary is shown in Fig. 8. Calibrations for potential and position are shown. The potential varied smoothly until the tip of the capillary hit the bottom of the pit as noted by the discontinuity followed by a smaller slope. The length of this region of smaller slope is assumed to be the displacement of the Luggin capillary into the Plexiglas bushing (Fig. 1) as the summation of these displacements from each run agreed with measurements made with the cathotometer. The potential on the outward traverse was slightly lower for a given tip position presumably due to disturbing the precipitate with the capillary. The pit current usually also increased during the outward traverse indicating a slight decrease in resistance.

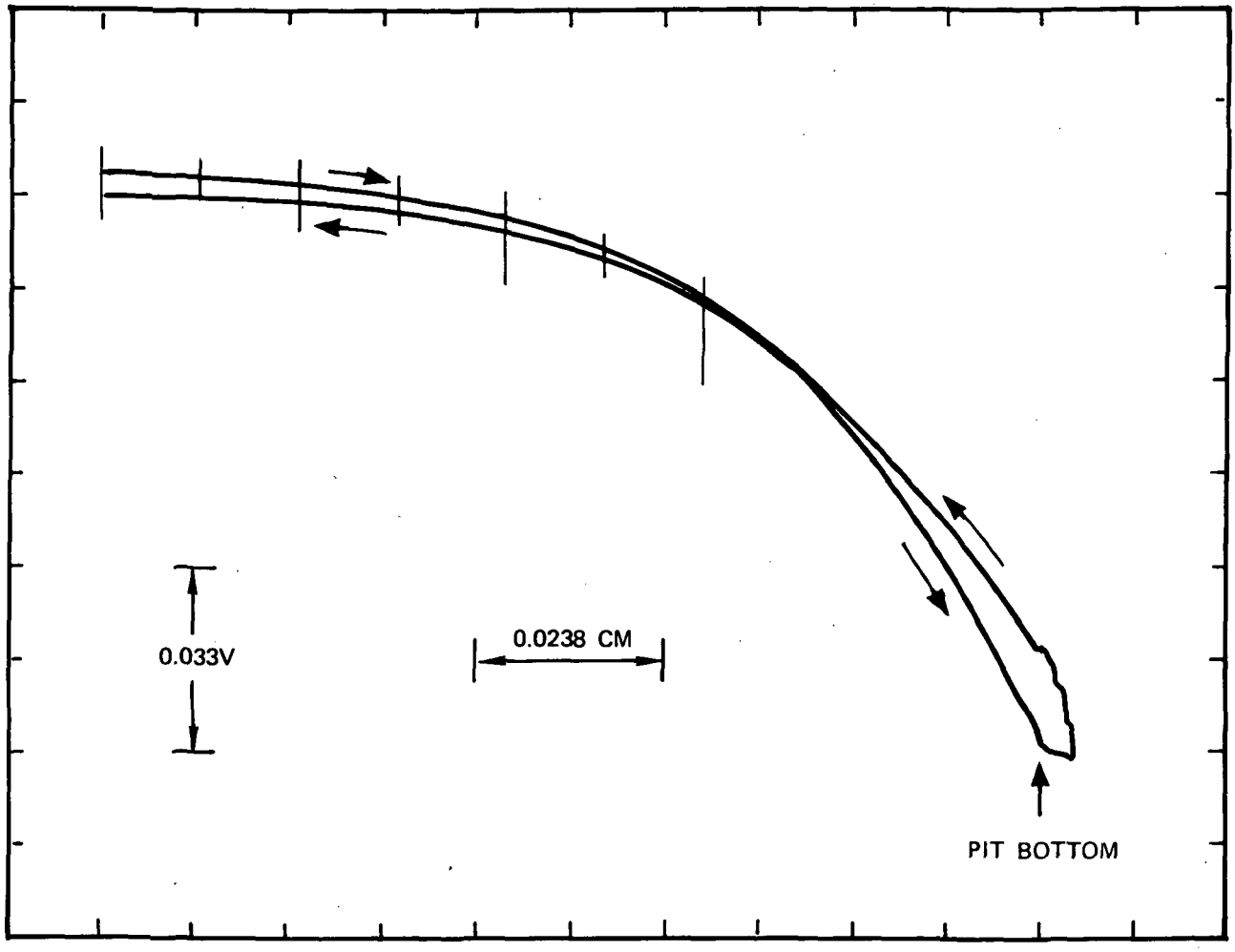

Fig. 8 - Potential Traverse in Pit (pit depth = 0.094 cm at this measurement) Tic Marks are 0.005 in Apart According to Micrometer.

Eleven usable traverses were obtained for the lower and upper plateau between 2.0 and 8.5 V applied. Five other runs were rejected because they were taken below 2.0 V, had an inadequate sensitivity or the curve was erratic. Slopes were determined for each usable curve and the electrolyte conductivity was calculated as a function of position by

$$\kappa = -\frac{i}{d\phi/d\ell} \tag{1}$$

using the current density i at the time of measurement. Values of κ were averaged as a function of position from the pit bottom and plotted in Fig. 9 with their standard deviations. Values for capillary-opening positions outside of the pit mouth were rejected from the averages. It is seen that conductivity decreases considerably within the pit and appears to become linear with distance from the bottom for small distances. The straight-line portion extrapolates to zero conductivity at a position equal to the distance of the capillary opening above the tip (Fig. 2) and has the equation

$$\kappa = 2.6\ell \tag{2}$$

Open-Circuit Potential Transients - Potential transient data replotted from oscilloscope photograhs and strip chart records are shown in Fig. 10. For applied potentials at 2.0 V through 5.0 V a linear relationship was obtained between open-circuit potential and logarithm of time from 10^{-6} sec. to 10^{-2} sec. At 7.0 V applied the linear region extended only about two decades of time. Below 2.0 V there did not appear to be any linear region.

A minimum occurred at about 10^{-1} sec. from open circuit for all applied potentials. The values of this minimum are shown in Fig. 11 for pits in 4.4 M HBr and 5 M HI. These were determined by visually observing the oscilloscope screen for repeated open-circuit transients. The minimum could be interpreted as either the potential of the corroding surface or a mixed potential established at open circuit.

4.2.3 Discussion

Potential Distribution - The first task is to account for the potential distribution in and around a pit. The potential drop outside of the pit

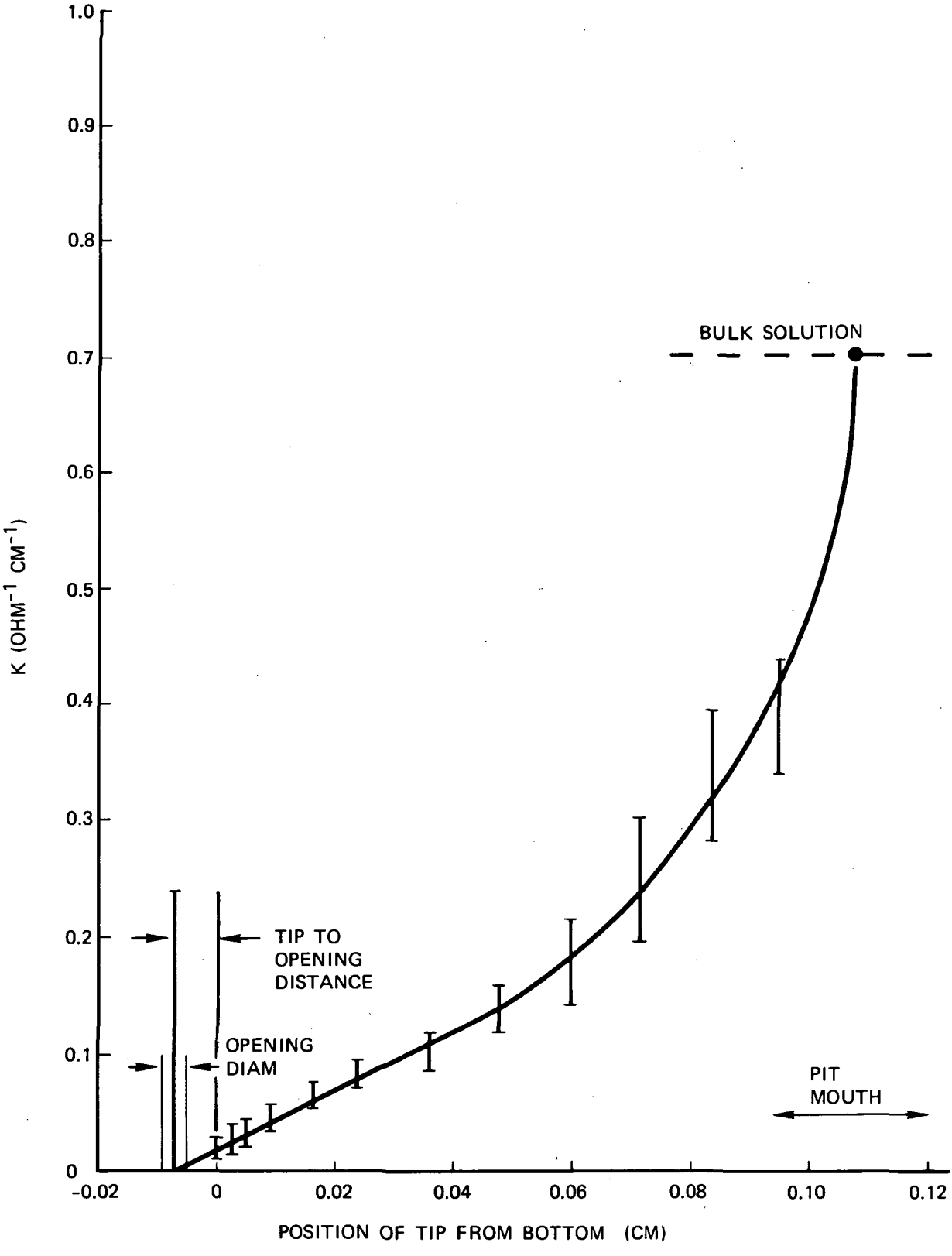

Fig. 9 - Electrolyte Conductivity in Pit.

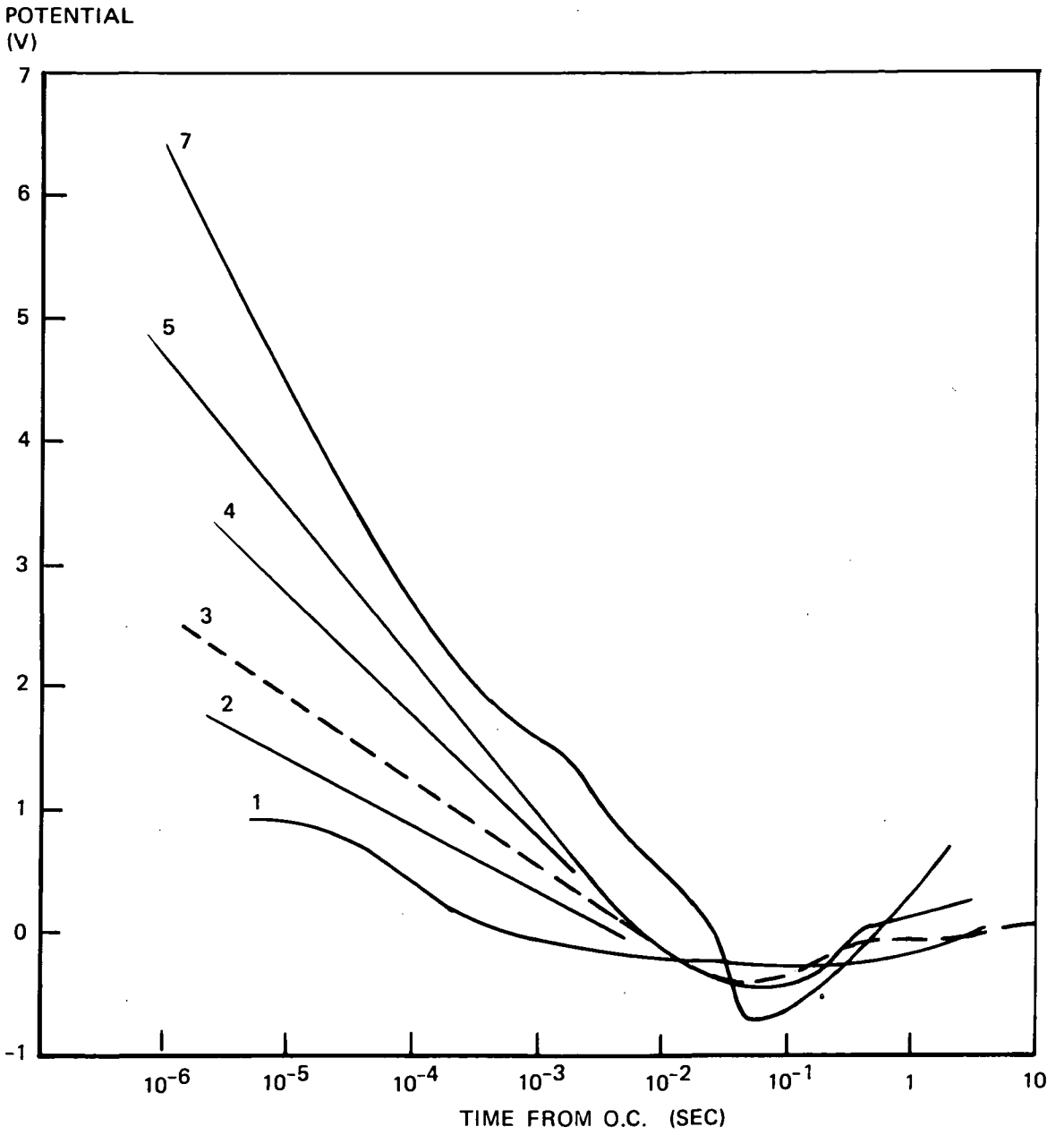

Fig. 10 - Open-Circuit Potential Transients for Titanium Pits in 4.4 M HBr Numbers on Curves are Initial Applied Potential (V).

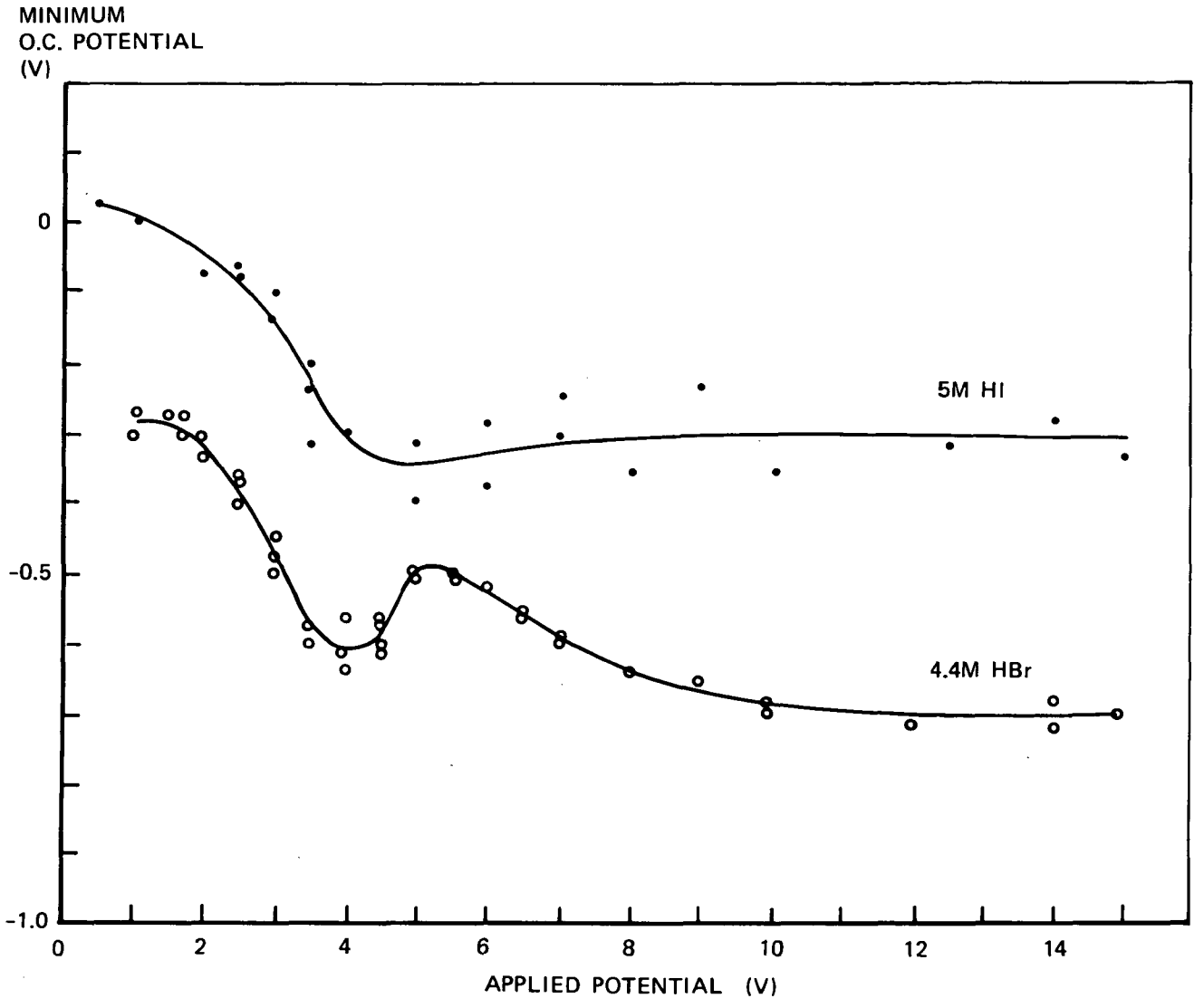

Fig. 11 - Minimum Open-Circuit Potentials for Titanium Pits in HBr and HI.

approximated by hemispherical conduction from an infinite distance to the pit mouth,

$$\Delta\phi_{oo} = \frac{ir}{\kappa}, \qquad (3)$$

is on the order of tens of millivolts for the current densities, pit radii and concentration (4.4 M HBr) used in the experiments. Measurements with the probe cell (Figure 1) were in agreement with this calculation. The metal surface is at a potential negative to the hydrogen electrode as demonstrated by hydrogen gas issuing from the pits in agreement with the minimum open circuit potentials of -0.3 to -0.7 V in HBr (Figure 11). Therefore, nearly all of the difference between the applied potential and this negative potential must be accounted for within the boundaries of the pit.

An approximation for the potential drop within the electrolyte of the pit is made by integrating Equation 1, using the linear conductivity relationship of Equation 2,

$$\Delta\phi_{oi} = \frac{i}{2.6} \ell n(\ell/\ell o) \qquad (4)$$

For a pit depth, ℓ = 0.1 cm and a lower bound distance of molecular dimensions, $\ell_o = 10^{-7}$ cm, $\Delta\phi_{oi} = 5.3i$. This is, of course, a gross extrapolation down to molecular dimensions but it will serve as a first approximation. Values of Equation 4 are shown in Table 2, together with applied potentials and current densities from the potential traverse experiments. It is seen that the largest component of potential by difference $\Delta\phi = \phi_p - \phi_{oc} - \Delta\phi_{oo} - \Delta\phi_{oi}$, is unexplained.

The unaccounted potential could be either due to error in the conductivity extrapolation or to presence of high field conduction in a thin salt film. A high activation overpotential could be excluded because hydrogen gas is produced.

Potential Decay - The potential decay experiments are diagnostic in that a linear relationship of potential with log time is characteristic of discharge of the electrical double layer by a reaction following Tafel kinetics (6,8)

or to discharge of a film capacitance by high-field conduction (9). The former gives a constant Tafel slope independent of the initial potential, whereas the latter gives a variable slope which is a function of the film thickness.

A plot of the decay slopes as a function of applied potential from 2 to 5 V is shown in Figure 12. The data appear to be linear and the least-squares line has a slope of -0.20 and an intercept of -0.55 V. The potential-decay data are therefore consistent with high-field conduction through a salt film; the intercept being the potential for zero salt film thickness and the slope equal to $-2.3\ \delta/\beta$ (9). Values of $-2.3\ \delta/\beta$ calculated for δ and β for various oxides (9) are in the range of -0.05 to -0.2.

Presence of a salt film is in accord with the observations of Frank (10) and Vetter and Strehblow (11) for pitting of iron.

Paradox - An apparent paradox exists in that the steady-state polarization data (Figures 3 and 4) indicate a diffusion limited process whereas the potential decay experiments indicate high-field conduction controlling. It will be assumed that both operate simultaneously and that they somehow have to be reconciled. One possibility is that they are parallel processes, e.g., a stoichiometric $TiOBr_2$ is formed at the electrode surface, the Br^- arriving by high-field conduction and water arriving by diffusion. A second possibility is that there are series processes, e.g., a salt film that maintains a thickness to use up by high-field conduction, the potential applied and that the rate of dissolution of this film is controlled by diffusion of water to the electrolyte-salt interface. The latter, considered to be more probable, will be examined in more detail.

Model - A qualitative model to describe the events in a pit will be presented here; the mathematical development will be presented in a subsequent paper. Figure 13 outlines the essence of the idea. A salt film is assumed to form on the metal surface. The simplest composition, TiX_4, is chosen as shown in Figure 13, although it could also be $TiOX_2$ or some other halide salt of Ti(IV). The halide ion is transported by high-field conduction through the salt to metal surface. The X^- ion occurs at a high concentration in the electrolyte next to the salt film because it is regenerated within the diffusion layer by

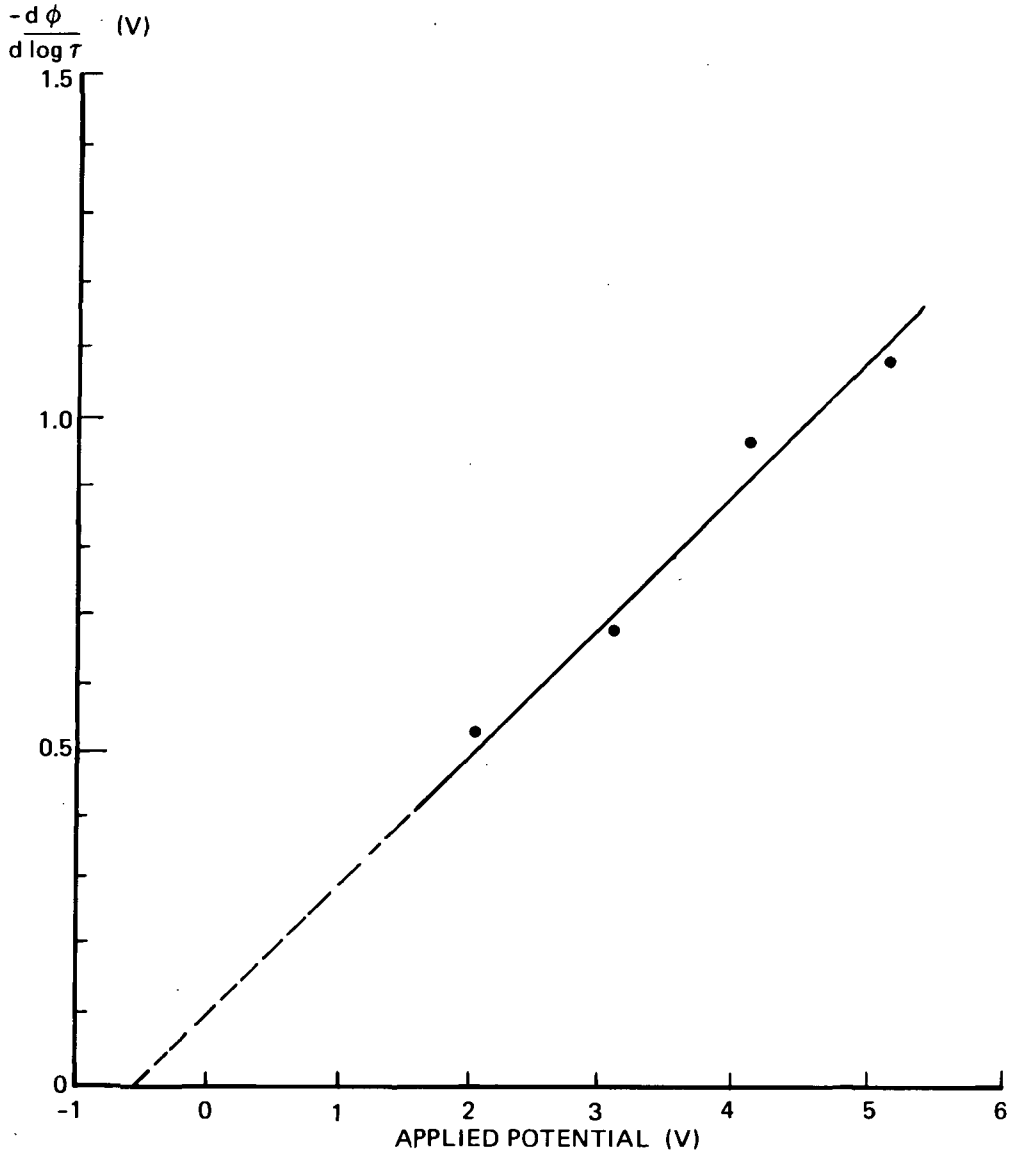

Fig. 12 - Slope of Potential-Decay Curves.

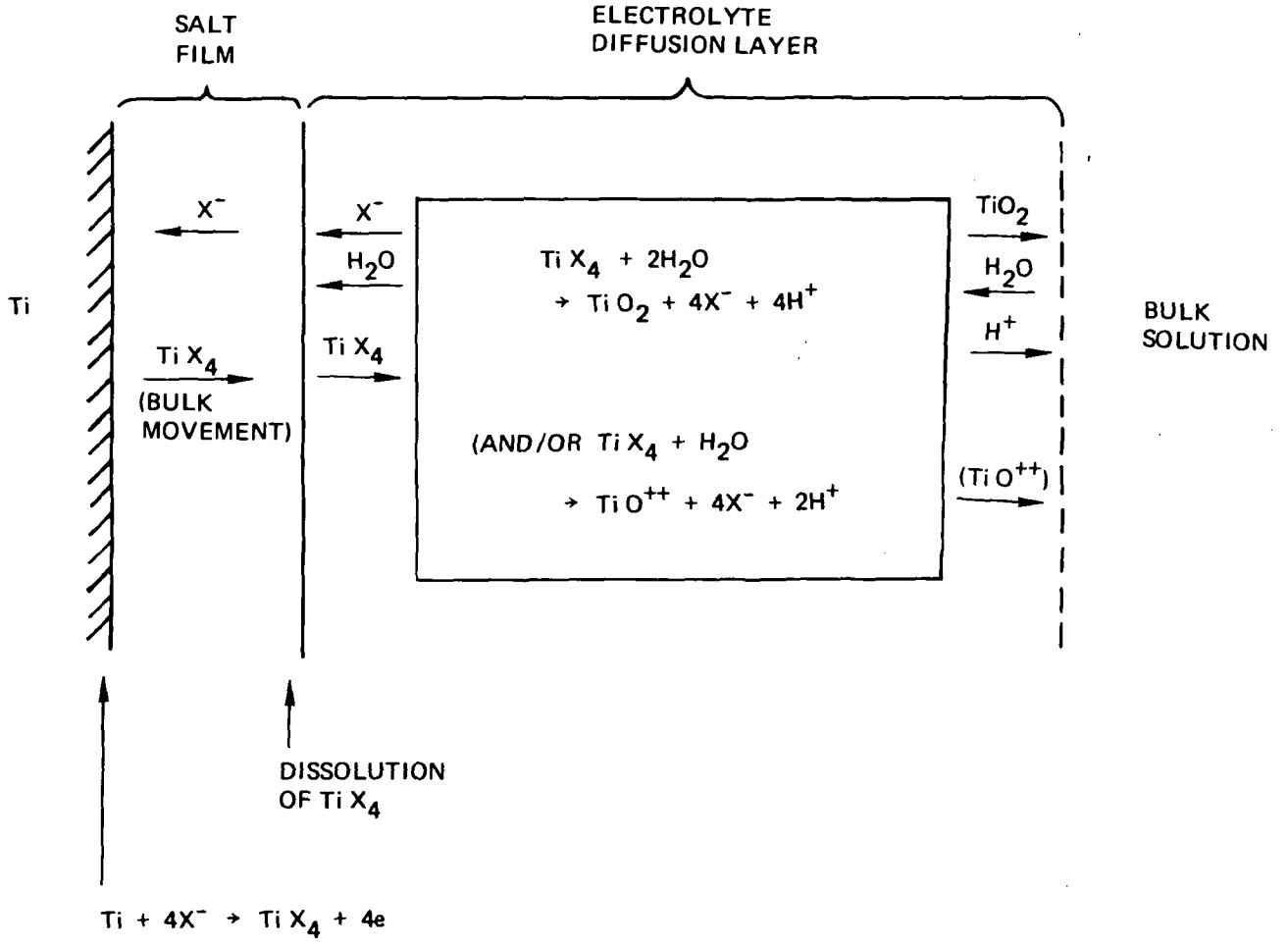

Fig. 13 - Model for Reactions in Pit.

hydrolysis of TiX_4. The salt is transported away from the metal-salt interface by bulk flow. (The alternative of high-field conduction of Ti^{4+} outward does not change the arguments presented here.)

At the salt-electrolyte interface the TiX_4 dissolves convalently in the water which has diffused to the interface. Within the diffusion layer, hydrolysis of TiX_4 to TiO_2 and/or TiO^{++} occurs, generating halide and hydrogen ions which make the solution acidic regardless of the pH of the bulk solution outside of the pit. If the hydrolysis goes to completion within the pit, the overall pit reactions are:

$$Ti + 2\ H_2O \rightarrow TiO_2 + 4\ H^+ + 4e$$

or

$$Ti + H_2O \rightarrow TiO^{++} + 2H^+ + 4e$$

and only TiO_2, TiO^{++} and H^+ are transported out. Water is then the only species transported into the pit from the environment at steady state.

Areas of agreement of the experimental data and the model can now be discussed, starting with the diffusion layer.

The orange viscous material deep in the pits in bromide solutions is consistent with the color of $TiBr_4$ or $TiOBr_2$ which would be an expected intermediate in the hydrolysis. White precipitate, at the outer part of the pits, and dense colorless liquid streaming out of the pits, are consistent with TiO_2 and TiO^{++} ion, respectively, expected from valence IV titanium.

Decrease in conductivity with distance into a pit may be attributed to an increase in viscosity due to high concentration of TiO_2 and TiO^{++}. Valence IV titanium has a known tendency to polymerize (12). The linear form of the decrease in conductivity with distance is yet to be understood quantitatively, however. Decrease in conductivity could not be attributed to concentration of conducting species in the model because both H^+ and X^- are generated in the diffusion layer and therefore should be at high concentration.

According to the model, the only species entering a pit at steady state is

water. If this is the diffusion limited species the current density would decrease with depth or thicker viscous layer. That the current density decreased in a variable way from 0 to -1.7 power of depth indicates a complex nature of the viscous layer. Increase in current density with stirring of the viscous layer is in accord with a diffusion limted species in it.

The relative independence of current density on pH in the bulk between 4.4 M HBr and 1 M KBr can be attributed to the pit generating its own acid environment by hydrolysis.

The rapidly increasing current density with temperatures above 50°C for the lower plateau in iodide solution can only be speculated upon at this time. It is known from TiO_2 pigment technology that nucleation and growth of TiO_2 particles from chloride or sulfate solutions occur above a temperature of 50-60°C (13) and that they are arrested below this temperature. Growth of TiO_2 particles in a pit could decrease the concentration of TiO^{++} and thus avoid the viscous polymeric gel.

The requirement for a salt film has already been discussed but the points will be summarized here. The fact that hydrogen gas issues from the pits is the strongest argument that the metal surface is at a negative potential. Hydrogen generation can be attributed to diffusion of hydrogen ions through the salt film. Electric migration tends to carry them out. The observation of increased hydrogen gas rate when the potential was decreased is consistent with a greater diffusion flux of hydrogen ions through a thinner salt film.

Faceting and terraces observed on the metal surface at the lower plateau and the residual differences between grains indicates that the metal is reacting at close to the reversible potential. The reversible potential for the reaction

$$Ti + 4Br^- \rightarrow TiBr_4 + 4e$$

is -0.76 V (SCE) according to thermodynamic data in Latimer (14). The minimum in the open-circuit potential (Figure 11) and the extrapolated intercept of the slopes of the potential decay curves (Figure 12) are in

approximate agreement with a mixed potential from this reaction and hydrogen ion reduction.

Most of the potential drop in a pit cannot be accounted in any other way than by high-field conduction in a salt film. The potential decay (Figure 10) and the constant double derivative of open-circuit potential to log time and applied potential (Figure 12) are in accord with a salt film concept.

Unresolved Questions - Although the model qualitatively is in accord with the experimental observations, several questions remain. The composition of the salt film is no known; whether it is TiX_4, $TiOX_2$ or other.

The explanation of two plateaus in current density is unknown. The ratio of current densities of the upper to the lower plateau in 8 experiments was 1.53 with standard deviation of ± 0.04. More work would have to be done to resolve which term in the diffusion equation changes by this amount.

The significance of the pitting potential is still elusive. The same value of pitting potential was obtained for the titanium pencils as was earlier determined for pitting on titanium foil (1). The same technique of decreasing potential of a propagating pit until the current decayed to zero was used. Pitting potential in an artificial pit at the end of a titanium pencil cannot be attributed to an equilibrium between a salt layer and a preexisting oxide at the boundary of a pit as there is no preexisting oxide layer present. However, salt and oxide or hydride films could possibly form simultaneously.

Explanation of the porous surface Figure 5) bearing no relation to the metal grains at potentials between the pitting potential and 1.5 to 2.0 V is also unresolved. To force dissolution to occur deep in holes or pores requires that the outer pore surface become passivated. Two possible passivating agents are TiO_2 and TiH_2. A way to passivate the outer part of a pore but not the inner part would be to have diffusion of passivating agent through a layer such that it reaches the peaks but not the valleys at a sufficient rate. This concept is related to action of smoothing agents in electroplating (15).

REFERENCES

1. T. R. Beck, NASA Contract NAS7-489 Quarterly Report No. 1, Sept. 1966.
2. H. J. Engell and N. D. Stolica, Z. Physik. Chem., 215, 167 (1960).
3. U. F. Frank, Werkstoffe und Korrosion, 9, 504 (1958).
4. H. Kaesche, Z. Physik. Chem., NF 26, 138 (1960).
5. H. F. Walton, J. Electrochem. Soc., 97, 219, (1950).
6. B. E. Conway, Electrode Processes, p. 155, Ronald Press, New York, 1965.
7. R. B. Bird, W. E. Stewart and E. N. Lightfoot, Transport Phenomena, p. 541, John Wiley, New York, 1960.
8. J. A. V. Butler and G. Armstrong,Trans. Faraday Soc., 29, 1261 (1933).
9. L. Young, Anodic Oxide Films, p. 33, Academic Press, New York, 1961.
10. U. F. Frank, 1st Int. Congr. on Metallic Corrosion, London 1961, p. 120, Butterworths, London, 1962.
11. K. J. Vetter and N. N. Strehblow, Paper No. 14, U. R. Evans Intl. Conference on Localized Corrosion, Williamsburg, Va., Dec. 1971.
12. F. A. Cotton and G. Wilkinson, Advanced Inorganic Chemistry, Interscience, New York, 1966.
13. J. Barksdale, Titanium, Its Occurance, Chemistry and Technology, 2nd Ed., Chap. 14 and 18, Ronald Press, New York, 1966.
14. W. M. Latimer, Oxidation Potentials, 2nd Ed., Prentice Hall, Englewood Cliffs., N. J., 1952.
15. O. Kardos and D. G. Foulke, Electrodeposition on Small-Scale Profiles, in Advances in Electrochem. and Electrochem. Engineering 2, Delahay and Tobias, Ed., John Wiley, New York, 1962.

Table 1. Volumetric Measurements with Gas Burette

	Gas Volume (cm^3)			
	1	1a	2	3
Gas from Pit (or cathode)	0.100	-	0.210	0.165
Loss on sparking	0.020	-	0.050	0.010
Remaining	0.080	-	0.160	0.155
H_2 added	0.027	-	-	-
Total	0.107	-	-	-
After sparking	0.107	-	-	-
O_2 added	0.031	0.025	-	-
Total	0.138	0.105	-	-
After sparking	0.080	0.047	-	-
Remaining at H_2-O_2 equivalence point for simultaneous O_2 addition and spark	-	-	0.095	0.070

NOTES:

1. Pitting in 1 M HCl; H_2 generated in 1 M HCl; O_2 generated in 1N H_2SO_4
2. Pitting in 1 M NaCl + 0.1 M NaOH, preboiled; O_2 generated in 0.3 M NaOH, preboiled
3. H_2 and O_2 generated in 0.3 M NaOH, preboiled.

Table 2. Calculation of Potential Drops in Pit

ϕ_p (V)	i (A/cm^2)	ϕ_{oc} (V)	$\Delta\phi_{oo}$ (V)	$\Delta\phi_{oi}$ (V)	$\Delta\phi = \phi_p - \phi_{oc} - \Delta\phi_{oc} - \Delta\phi_{oi}$, unaccounted (V)
1	0.005	-0.28	-	0.03	1.25
1.5	0.06	-0.28	-	0.32	1.46
2	0.11	-0.40	0.01	0.58	1.81
3	0.12	-0.48	0.01	0.64	2.47
4	0.11	-0.62	0.01	0.58	4.03
5	0.18	-0.50	0.02	0.95	4.53
8.5	0.25	-0.65	0.03	1.33	7.79